Organic &
Biomolecular Chemistry

PAPER

Diels–Alder reactions of 4-halo masked *o*-benzoquinones. Experimental and theoretical investigations†

Cite this: *Org. Biomol. Chem.*, 2014, **12**, 5656

Seshi Reddy Surasani, Santosh Kumar Reddy Parumala and Rama Krishna Peddinti*

The studies on [4 + 2] cycloaddition of 4-halo derivatives of 6,6-dimethoxycyclohexa-2,4-dienones known as orthoquinone monoketals/masked *o*-benzoquinones are described. The 4-fluoro, 4-chloro- and 4-iodo-masked *o*-benzoquinones were stable enough for their isolation and characterization. These conjugated dienones cycloadded with several electron-deficient and electron-rich dienophiles in a highly regio- and stereo-selective manner to afford the corresponding halo bicyclo[2.2.2]octenone derivatives in high to excellent chemical yields. The halo masked *o*-benzoquinones did not undergo dimerization under the reaction conditions. To evaluate the observed selectivities of these Diels–Alder reactions, we have performed quantum mechanical calculations for the reactions between halo masked *o*-benzoquinones and methyl vinyl ketone and ethyl vinyl ether at the B3LYP/6-31G** theory level. The differences in HOMO and LUMO energy gaps suggest that these reactions can be classified as inverse electron-demand Diels–Alder reactions. The calculated transition state energies and global electronic indexes supported the experimentally observed selectivities of the reaction in many cases.

Received 2nd May 2014,
Accepted 19th May 2014

DOI: 10.1039/c4ob00856a

www.rsc.org/obc

Introduction

Oxidative dearomatization of aromatic compounds has been widely identified as a powerful tactic for the generation of high levels of molecular complexity from easily accessible starting materials. Of particular prominence is the dearomatization of methoxyphenols into cyclohexadienone synthons.[1] The electron-rich aromatic compounds such as 2-methoxy- or 4-methoxy-phenols, which are nucleophilic in nature, can undergo oxidative dearomatization to generate electrophilic intermediates by chemical or electrochemical process. Thus the oxidation of 2-methoxyphenols in the presence of alcohols such as methanol generates highly reactive conjugated cyclohexadienones better known as orthobenzoquinone monoketals or masked *o*-benzoquinones (MOBs), which can be trapped often with dienophiles in Diels–Alder reactions to furnish the adducts with excellent stereo- and regio-selectivity (Scheme 1).[2,3] Liao exploited the Diels–Alder strategy of MOBs for the synthesis of bicyclo[2.2.2]octenones, oxatricycles, triquinanes and bicyclo[4.2.2]decenones that are pivotal synthons in the construction of natural products with diverse structural nature.[3] The most recent examples of total synthesis based on the MOB strategy are (±)-eremopetasidione,[4] the tetracyclic lycopodium alkaloid (±)-magellanine,[5] the sesterpenic acids (±)-bilosespenes A and B,[6] polyfunctionalized *cis*-decalins,[7] (±)-penicillones A and B,[8] (±)-3β-angeloyloxyfuranoeremophilane and (±)-3β methacryloyloxyfuranoeremophilane,[9] (±)-annuionone B and (±)-tanarifuranonol,[10] optically active condurамines,[11] helisorin, helicterin B and helisterculin A, and neolignans.[12]

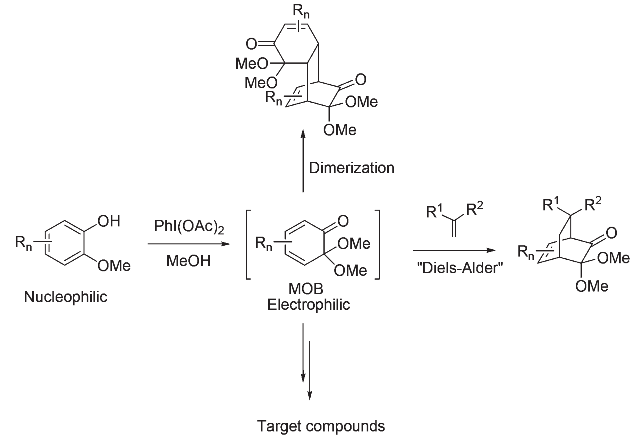

Scheme 1 Generation and reactivity of masked *o*-benzoquinones.

Department of Chemistry, Indian Institute of Technology, Roorkee-247 667, Uttarakhand, India. E-mail: rkpedfcy@iitr.ernet.in, ramakpeddinti@gmail.com; Fax: (+) 91 13 3227 3560; Tel: (+) 91 13 3228 5438

† Electronic supplementary information (ESI) available: NMR data tables, copies of ^{1}H and ^{13}C NMR spectra, copies of 2D NMR spectra, crystallographic data, theoretical data and transition state structures and theoretical Cartesian coordinates. CCDC 815225 and 900005. For ESI and crystallographic data in CIF or other electronic format see DOI: 10.1039/c4ob00856a

The bicyclo[2.2.2]octenone derivatives are versatile synthons and can be converted to various bicyclic and tricyclic intermediates.[3] Further, bicyclo[2.2.2]octenones experience intriguing and useful photochemical reactions, such as 1,3-acyl migration and oxa-di-π-methane rearrangement.[13] The most privileged protocol for the synthesis of these bicyclo[2.2.2]octenones is the Diels–Alder reaction of cyclohexa-2,4-dienones with dienophilic compounds.

The *in situ* generated MOBs undergo Diels–Alder reactions with external dienophiles to furnish bicyclo[2.2.2]octenone derivatives in high to excellent chemical yields.[14] In the absence of an external dienophile, these reactive species possessing dienic and dienophilic moieties undergo self-dimerization through Diels–Alder reactions. The dimerization can be hindered by replacing one of the methoxy groups at C-6 by acetoxy functionality. The reactivity of the masked *o*-benzoquinones can be modulated by careful substitution on the carbo-diene system and/or by tuning the substituents on the C-6 carbon. The nature of the substituents and substitution pattern is often critical in determining the reactivity and stability of these MOBs. The MOBs containing substitution of any nature (*e.g.*, alkyl, alkoxy, ester, and halo) at position 5 are non-dimerizing and stable.[15] The parent MOB derived from guaiacol and MOBs bearing electron-withdrawing groups on position 4 are very reactive and dimerize spontaneously and provide the corresponding MOB dimers.[14] The functionalities such as alkyl and bulky groups such as *tert*-butyl and acetal on position 4 retard the dimerization event.[14–16]

The substitution of halogen at position 4 is another strategy to diminish the MOB self-dimerization. Andersson and Berntsson observed the non-dimerizing 4-iodo MOB.[17] Liao used bromine at position 4 to retard the dimerization and carried out Diels–Alder cycloaddition with dienophiles bearing electron-withdrawing groups.[7] Patrick used fluorine at position 4 of MOB during his work on the [4 + 2] cycloaddition reactions.[18] In the course of remarkable work on arene oxidations, Quideau used bromo substitution to isolate stable MOBs.[19] In our laboratory we have isolated the 4-halo MOBs for their characterization.[20] During our studies on the Diels–Alder reaction of 4-halo MOBs with a series of electron-deficient and electron-rich dienophiles for the synthesis of highly selective halo-substituted bicyclo[2.2.2]octenone derivatives, we did not observe the dimeric Diels–Alder adducts by self-dimerization of 4-halo MOBs.[20b,c] In order to understand the observed selectivities in the Diels–Alder reaction of 4-halo MOBs, we carried out quantum mechanical DFT calculations. Herein we present a detailed account of our studies on the title reactions[20b,c] together with theoretical treatment for the validation of the experimental results.

Results and discussion

Intrigued by the non-dimerizing nature of 4-halo MOBs, we became interested in evaluating the stability of 4-halo MOBs by isolation. As a prelude to this objective, we treated 4-fluoroguaiacol with diacetoxyiodobenzene (DAIB) in methanol at 0 °C. Thus a solution of DAIB (1.1 equiv.) in methanol was added to a solution of 4-fluoroguaiacol (**1**) in methanol at 0 °C under stirring. The solution turned immediately into yellow indicating the formation of MOB **5**. After 10 min of stirring at the same temperature, the contents were concentrated under vacuum and the residue was subjected to flash chromatography on silica gel to furnish a yellow liquid. The ^{1}H NMR for the sample was recorded. The spectrum revealed no traces of a dimeric compound. Similarly, 4-chloroguaiacol (**2**) and 4-iodoguaiacol (**4**) were also oxidized to the corresponding MOBs **6** and **8**. The Diels–Alder reaction of the diene **5** with methyl acrylate (MA, 25 equiv.) was carried out at room temperature. The reaction was complete in 24 h and after usual work-up and column chromatographic purification, the cycloadduct **9a** was isolated in an overall yield of 59% in two steps. To shorten the process, we then applied a one-pot oxidative ketalization/Diels–Alder protocol by generating the MOB **5** *in situ* in the presence of the dienophile. Thus the oxidation of methoxyphenol **1** was performed with slow addition (30 min) of a methanolic solution of DAIB (1.1 equiv.) in the presence of MA (25 equiv.) at 0 °C. After 10 min of time the ice-bath was removed and the contents were stirred at room temperature for 24 h (Method A) to isolate the adduct **9a** in 61% yield. To gain rapid access to **9a**, the MOB **4** was generated at 50 °C in the presence of methyl acrylate (Method B). The reaction was complete in 1 h and in this process the adduct **9a** was isolated in 72% yield. Encouraged by results from the reaction of phenol **1** with MA, we carried out the oxidative ketalization/Diels–Alder reactions of **1** with electron-deficient methyl methacrylate (MMA) and methyl vinyl ketone (MVK) following the procedure detailed in methods A and B (Scheme 2, Table 1). All these adducts **9a–c** were obtained as single isomers as indicated by the ^{1}H NMR of the crude reaction mixtures. However, not to our surprise, the Diels–Alder reaction of MOB **5** with acrylonitrile (ACN) under similar conditions provided the

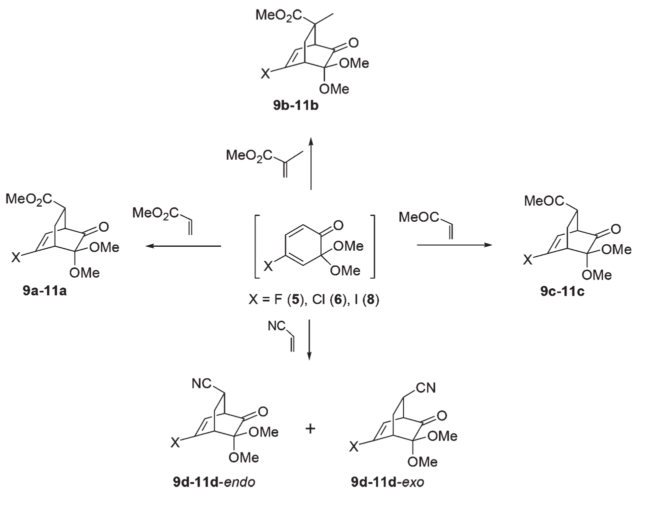

Scheme 2 Diels–Alder reactions of 4-halo MOBs with electron-deficient dienophiles.

Table 1 Diels–Alder reactions of halo-MOBs **5**, **6** and **8** generated from 4-halo-guaiacols **1**, **2** and **4**[a]

Entry	4-Halo-2-methoxy-phenol	MOB	Dienophile	Method[b]/time[c]	Product	Yield[d] (%)
1	**1**	**5**	MA	A/24 h	**9a**	61
2	**1**	**5**	MA	B/1 h	**9a**	72
3	**1**	**5**	MMA	A/24 h	**9b**	50
4	**1**	**5**	MMA	B/1 h	**9b**	61
5	**1**	**5**	MVK	A/24 h	**9c**	89
6	**1**	**5**	MVK	B/1 h	**9c**	91
7	**1**	**5**	ACN	A/24 h	**9d**	57[e]
8	**1**	**5**	ACN	B/1 h	**9d**	60[e]
9	**2**	**6**	MA	A/24 h	**10a**	77
10	**2**	**6**	MA	B/1 h	**10a**	92
11	**2**	**6**	MMA	A/24 h	**10b**	64
12	**2**	**6**	MMA	B/1 h	**10b**	72
13	**2**	**6**	MVK	A/24 h	**10c**	70
14	**2**	**6**	MVK	B/1 h	**10c**	78
15	**2**	**6**	ACN	A/24 h	**10d**	70[e]
16	**2**	**6**	ACN	B/1 h	**10d**	80[e]
17	**4**	**8**	MA	A/44 h	**11a**	80
18	**4**	**8**	MA	B/1 h	**11a**	97
19	**4**	**8**	MMA	A/47 h	**11b**	81
20	**4**	**8**	MMA	B/1 h	**11b**	90
21	**4**	**8**	MVK	A/28 h	**11c**	76
22	**4**	**8**	MVK	B/1 h	**11c**	85
23	**4**	**8**	ACN	A/24 h	**11d**	91[e]
24	**4**	**8**	ACN	B/1 h	**11d**	93[e]

[a] The reactions were carried out with 1 mmol of halo-guaiacol, 25 mmol of dienophile and 1.1 mmol of DAIB in 10 mL of MeOH. [b] Method A: room temperature; Method B: 50 °C (see the Experimental section). [c] Represents the reaction time after the addition of DAIB. [d] Yield of pure and isolated products. [e] Mixture of stereoisomers.

cycloadduct **9d** as a mixture of *endo*- and *exo*-stereoisomers in a 2.2 : 1 (Method A) ratio. The non-selective Diels–Alder reactions of MOBs with ACN are known in the literature.[21]

To broaden the scope of this reaction, we carried out reactions of 4-chloro and 4-iodoguaiacols (**2** and **4**) with MA, MMA, MVK and ACN at room temperature as well as at 50 °C (Methods A and B) (Scheme 2). The results are presented in Table 1. The yields of the cycloadducts **9a–c–11a–c** are comparable to those adducts derived from 4-bromo MOB (**7**) of 4-bromoguaiacol (**3**).[7b] The reactions carried out at 50 °C provided the products in slightly higher yield. The reactions of 4-iodoguaiacol (**4**) performed at room temperature required longer reaction times (24–47 h). As in the case of 4-fluoro MOB (**5**), the reactions of 4-chloro and 4-iodo MOBs (**6** and **8**) with ACN furnished the products **10d** and **11d** as mixtures of *endo*- and *exo*-stereoisomers in 1 : 1.4 and 1.1 : 1 ratios, respectively.

The MOBs are known for their Diels–Alder reactivity both with electron-deficient[7a,14,15b] and electron-rich[22] dienophiles. Plumet[22d] and Liao[22a–c] reported the inverse electron-demand Diels–Alder (IEDDA) reactions of MOBs. Encouraged by the results obtained from the Diels–Alder reactions of *in situ* generated 4-halo MOBs with electron-deficient dienophiles, we then turned our attention to inverse electron-demand Diels–Alder reactions of these MOBs. The DAIB mediated oxidation of 4-fluoro-2-methoxyphenol in the presence of styrene, a conjugative dienophile, provided the Diels–Alder adduct **12a** in 65% yield. However, the reaction of **1** in the presence of ethyl vinyl ether or butyl vinyl ether in methanol under oxidative ketalization/Diels–Alder reaction conditions at room temperature furnished the corresponding cycloadducts in very low yields. In contrast, the chloro MOB **6** derived from chlorophenol **2** underwent efficient [4 + 2] cycloaddition with styrene, dihydrofuran (DHF), ethyl vinyl ether (EVE), butyl vinyl ether (BVE) and phenyl vinyl sulfide (PVS) to give the adducts **13a–e**, respectively (Scheme 3, Table 2). Though the Diels–Alder reaction between MOB **6** and vinyl acetate (VA) performed at room

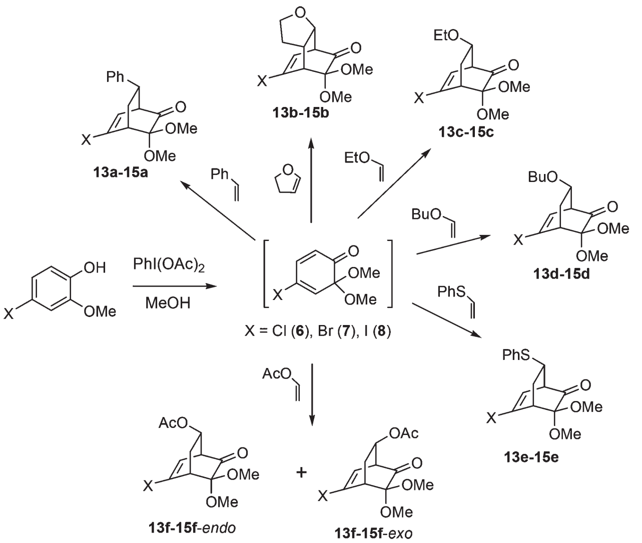

Scheme 3 Diels–Alder reactions of halo-MOBs with electron-rich dienophiles.

Table 2 Inverse electron-demand Diels–Alder reaction of halo-MOBs **5–8** generated from 4-halo-guaiacols **1–4**[a]

Entry	4-Halo guaiacol	MOB	Dienophile	Time[b]	Product	Yield[c] (%)
1	**1**	**5**	Styrene	20 h	**12a**	65
2	**2**	**6**	Styrene	20 h	**13a**	89
3	**2**	**6**	DHF	20 h	**13b**	90
4	**2**	**6**	EVE	2 h	**13c**	75
5	**2**	**6**	BVE	5 h	**13d**	82
6	**2**	**6**	PVS	20 h	**13e**	83
7	**2**	**6**	VA	24 h	**13f**	70[d]
8	**3**	**7**	Styrene	20 h	**14a**	74
9	**3**	**7**	DHF	20 h	**14b**	95
10	**3**	**7**	EVE	2 h	**14c**	77
11	**3**	**7**	BVE	5 h	**14d**	85
12	**3**	**7**	PVS	20 h	**14e**	77
13	**3**	**7**	VA	24 h	**14f**	90[d]
14	**4**	**8**	Styrene	20 h	**15a**	75
15	**4**	**8**	DHF	20 h	**15b**	85
16	**4**	**8**	EVE	2 h	**15c**	87
17	**4**	**8**	BVE	5 h	**15d**	88
18	**4**	**8**	PVS	20 h	**15e**	91
19	**4**	**8**	VA	24 h	**15f**	90[d]

[a] The reactions were carried out with 0.5 mmol of halo-guaiacol, 10 mmol of dienophile and 0.6 mmol of DAIB in 5 mL of MeOH. [b] Represents the reaction time after the addition of DAIB. [c] Yields of pure and isolated products. [d] Mixture of stereoisomers.

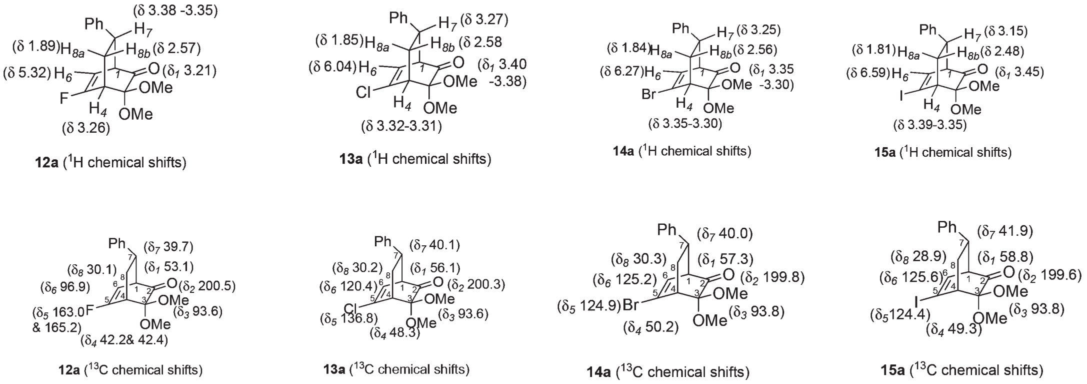

12a (^{1}H chemical shifts) **13a** (^{1}H chemical shifts) **14a** (^{1}H chemical shifts) **15a** (^{1}H chemical shifts)

12a (^{13}C chemical shifts) **13a** (^{13}C chemical shifts) **14a** (^{13}C chemical shifts) **15a** (^{13}C chemical shifts)

Scheme 4 Selected ^{1}H and ^{13}C chemical shifts (in ppm) of Diels–Alder adducts **12a–15a**.

temperature was regioselective, it was non-stereoselective. The product **13f** was obtained as a 1 : 5 mixture of *endo*- and *exo*-isomers. The cycloaddition reactions of *in situ* generated 4-bromo and 4-iodo MOBs **7** and **8** with the above dienophiles proceeded smoothly to afford the products **14a–e–15a–e** in very good to excellent chemical yields with excellent stereo- and regio-selectivities. The Diels–Alder reactions of VA with MOBs **7** and **8** at room temperature produced adducts **14f** and **15f** as 1 : 1.2 and 1 : 1.1 mixtures of *endo*- and *exo*-isomers, respectively. The non-selective Diels–Alder reactions of MOBs with VA are known in the literature.[23]

The structures of all the new compounds were assigned on the basis of their IR, ^{1}H NMR (500 MHz) and ^{13}C NMR (125 MHz) and DEPT, and mass spectral analyses. The cycloadducts displayed IR absorptions at 1734–1740 cm^{-1}, a characteristic absorption of the carbonyl function of bicyclo[2.2.2]-octenones derived from MOBs. In the ^{1}H NMR of adducts bearing Cl, Br and I substitutions, the vinylic proton resonates in the range of 5.97 to 6.66 ppm, whereas those of fluoro adducts resonate at 5.28 to 5.36 ppm. In general, the bridgehead proton H-1 of C-1, which is situated between the carbonyl carbon C-2 and the vinylic carbon C-6, resonates at higher frequency in comparison with the bridgehead proton H-4 of C-4. Of the two methylene protons on C-8, which is connected to C-4, the H-8a resonates in the range of 1.44–2.11 ppm.

The proton H-8b resonates at downfield (2.22–2.61 ppm) due to the deshielding effect of methoxy groups on C-3 carbon. In the ^{13}C NMR of these cycloadducts, the ring carbonyl carbon C-2 appears in the range of 199–205 ppm (Scheme 4). The ketal quaternary carbon C-3 appears in the skeletal range of 93.0–94.2 ppm. Among the bridgehead carbons C-1 and C-4, the former which is positioned next to the ring carbonyl resonates downfield. The effect of halogen atoms is clearly visible on the chemical shifts of C-4, C-5 and C-6. The C-4 appears at around 42, 48, 49 and 52 ppm in fluoro, chloro, bromo and iodo adducts, respectively. The halogen attached quaternary sp^2 carbon C-5 of these compounds resonates at about 164, 136, 124, 95 ppm, respectively. The sp^2 methine carbon C-6 of these halo-bicyclo[2.2.2]octenones resonates at around 97, 120, 124 and 134 ppm, respectively (Table 3).

Table 3 Selected ^{13}C chemical shifts (in ppm) of Diels–Alder adducts

Cycloadducts	C-4	C-5	C-6
F-adducts	41–42	164	97–99
Cl-adducts	47–48	135–137	119–122
Br-adducts	49–50	123–125	124–126
I-adducts	51–53	93–96	133–136

The substantial downfield shift of C-5 (~164 ppm) of fluoro adducts relative to sp^2 carbon of an olefin can be attributed to the deshielding effect of strong electronegativity of the fluorine atom. A less pronounced deshielding effect can be seen in chloro cycloadducts ($\delta_{\text{C-5}}$ up to 137 ppm) due to less electron withdrawal character of the chlorine atom in comparison with the fluorine atom. The chemical shifts of carbon C-5 of bromo compounds excellently mirror the almost nullified deshielding effect of the bromine atom due to its increased atomic size and reduced electronegativity. Owing to the well-known 'heavy-atom effect' of iodine, the monovalent iodocompounds provide a strong shielding effect on the geminal carbon and this is reflective of the diminished chemical shifts of carbon C-5 of iodo adducts. A marked deshielding effect on carbons C-4 and C-6 of iodo compounds is apparent on inspection of the data.

The geminal carbons C-5 of fluoro adducts displayed $^1J_{\text{CF}}$ coupling constants of about 282 Hz, whereas the $^2J_{\text{CF}}$ coupling constants of C-4 and C-6 are in the range of 21 and 9 Hz, respectively. The carbon C-1 is weakly coupled with fluorine with a $^3J_{\text{CF}}$ coupling constant of ~6 Hz. No coupling between the carbon C-3 and fluorine was observed in most of the fluoro adducts (Table 4). The listed carbon and fluorine coupling constants are in complete agreement with the expected values.

Table 4 ^{13}C–^{19}F coupling constants (in Hz) of fluoro adducts

Fluoro adduct	C-5 ($^1J_{\text{CF}}$)	C-4 ($^2J_{\text{CF}}$)	C-6 ($^2J_{\text{CF}}$)	C-1 ($^3J_{\text{CF}}$)	C-3 ($^3J_{\text{CF}}$)
9a	285.0	21.25	8.75	6.25	2.5
9b	282.5	21.25	8.75	6.25	0
9c	282.5	20.00	10.0	6.25	0
12a	282.5	22.50	8.75	6.25	0

The assignments of proton and carbon chemical shifts and stereochemical assignments are based on the collective information collected from proton–proton decoupling experiments, DEPT analysis, and 2D NMR experiments such as ^1H–^1H COSY, heteronuclear multiple quantum correlation (HSQC), heteronuclear multiple bond correlation (HMBC) and rotational frame nuclear Overhauser effect spectroscopy (ROESY) measurements. The data obtained from the 2D NMR experiments carried out on samples of Diels–Alder adducts **11c** and **14c** are presented in ESI.† The correlation between protons H_1–H_6, H_7–H_{8a} and H_{8a}–H_{8b} is clearly visible from ^1H–^1H COSY spectra. The CH connectivities between C_1–H_1, C_4–H_4, C_7–H_7 and C_8–H_8 are revealed by HMQC spectra. The HMBC analysis provides diagnostic proton–carbon correlations over multiple bonds which were found to be extremely helpful in the conformation of the structure of the product.

The Diels–Alder reactions of masked *o*-benzoquinones are highly stereo- and regio-selective and produce a single diastereomer. Of the four possible isomers, only the one possessing *ortho* regiochemistry (the electron-withdrawing/electron-releasing group is adjacent to the octenone carbonyl function) and *endo* stereochemistry (the electron-withdrawing/electron-releasing group is *anti* to the octenone carbonyl function) was formed in the current study (except the reactions with acrylonitrile and vinyl acetate).

The regiochemistry of the Diels–Alder adducts was deduced from ^1H–^1H decoupling NMR experiments. The assigned *endo* stereochemistry is corroborated by the coupling constants between H_7–H_{8b} and H_7–H_{8a} (Table 5). The data reveal that the coupling constants between H_7–H_{8a} are less than those of H_7–H_{8b}. The larger J value for H_7–H_{8b} reveals the *cis* orientation of the protons H_7 and H_{8b}, thus confirming the *endo* stereochemistry of the [4 + 2] cycloadduct. The *endo* stereochemistry of cycloadducts **11c** and **14c** was further confirmed by ROESY measurements. The assigned *ortho* and *endo* selectivities of compounds **14e** and **15a** were further confirmed from the single crystal X-ray structures.

Table 5 Chemical shifts (in ppm) of H_{8a} and H_{8b} and coupling constants (in Hz) between H_7–H_{8a} and H_7–H_{8b} of cycloadducts **9–15**

Compound	δ_{8a}	δ_{8b}	JH_7–H_{8a}	JH_7–H_{8b}
9a	2.11	2.29	5.5	10.0
9c	2.06	2.22	6.0	10.0
10a	2.02	2.34	5.5	10.5
10c	1.92	2.30	6.0	10.0
11a	1.95	2.26	6.0	10.0
11c	1.84	2.24	6.0	10.0
12a	1.89	2.57	7.5	10.5
13a	1.85	2.58	6.5	9.5
13c	1.56	2.46	7.0	8.0
13d	1.55	2.45	6.5	8.0
13e	1.49	2.60	5.0	9.0
14a	1.84	2.56	6.5	9.5
14c	1.55	2.45	6.0	8.5
14d	1.54	2.44	6.5	8.0
14e	1.49	2.60	6.0	9.5
15a	1.81	2.48	6.5	9.5
15c	1.52	2.38	7.0	8.5
15d	1.50	2.36	7.0	8.0
15e	1.48	2.54	5.5	9.5

In order to contribute to a better understanding of the influence of halogen atoms on position 4 of MOBs and to validate the experimentally obtained results, we then performed theoretical calculations using density functional theory (DFT) with the well-established B3LYP/6-31G** method.

Computational details

All the calculations were performed with the GAUSSIAN 09 suite of programs.[24] The geometries of all structures and transition states (TSs) were fully optimized with density functional theory[25] at the B3LYP/6-31G** level.[26] The theory has been shown to reliably predict the results of Diels–Alder and other pericyclic reactions.[27] A dielectric constant of 32.6 was used to simulate the methanolic environment. The stationary points were characterized by frequency calculations in order to verify that the TS had one and only one imaginary frequency. Further, intrinsic reaction coordinate (IRC) calculations were carried out at the same level to authenticate the transition states.

The regio-selectivity of Diels–Alder cycloaddition reactions of dienic MOBs with dienophiles MA/MVK and methyl vinyl ether/EVE has been analyzed in terms of frontier molecular orbital (FMO) theory.[14,28] To classify these cycloadditions in terms of normal- or inverse electron-demand Diels–Alder reactions, the calculations were performed on MOBs bearing substituents such as 4-Me, 4-CO_2Me, 4-COMe with MA/MVK at *ab initio* HF/3-21G* and HF/6-31G* calculations, and borderline energy gaps were obtained, rendering the prediction complicated.[14,28] The DFT at the B3LYP level with 6-31G basis set studies on Diels–Alder reactions has received much attention since the experimental results are in good agreement with them.[29,30] Consequently, we have calculated the energy levels of the HOMO and LUMO of halo MOBs and the dienophiles MVK and EVE by DFT calculations at the B3LYP/6-31G** level of theory. The calculated HOMO and LUMO energies of these 4π and 2π components are provided in ESI.†

The differences between $HOMO_{MOB}$ and $LUMO_{dienophile}$ are in the range of 5.15–5.43 and 7.87–8.15 eV for the reactions involving MVK and EVE, respectively. The differences between $HOMO_{dienophile}$ and $LUMO_{MOB}$ are in the range of 3.79–4.22 and 3.14–3.57 eV for the reactions of MVK and EVE, respectively (Table 6). Since the interactions between $HOMO_{dienophile}$ and $LUMO_{diene}$ are preferred, these reactions can be classified as inverse electron-demand Diels–Alder reactions. The difference in energy gaps ($\Delta\Delta E$) between two possible interactions is about 1 eV (with MVK) and about 4.5 eV (with EVE). The lesser $\Delta\Delta E$ values in the former are expected since both dienes and dienophiles are electron-deficient. These results indicate that the 4-halo MOBs undergo inverse electron-demand Diels–Alder reactions with both electron-rich as well as electron-deficient dienophiles.

Energies of transition structures

The reactions between (i) halo-MOBs and the electron-deficient dienophile MVK and (ii) halo-MOBs and the electron-

Table 6 DFT B3LYP/6-31G** energy gaps (E_v) between the relevant frontier orbitals for MOBs **5–8** and dienophiles MVK and EVE

Entry	Diene	Dienophile	NED $HOMO_{MOB}$–$LUMO_{dienophile}$	IED $HOMO_{dienophile}$–$LUMO_{MOB}$	Difference (NED – IED) $\Delta\Delta E$	Preferred interaction
1	FMOB	MVK	5.153332808	4.215621072	0.93771174	IED
2	ClMOB	MVK	5.224899316	4.121468936	1.10343038	IED
3	BrMOB	MVK	5.204218500	4.126911256	1.07730724	IED
4	IMOB	MVK	5.430619012	3.787038372	1.64358064	IED
5	FMOB	EVE	7.86959472	3.569889805	4.29970492	IED
6	ClMOB	EVE	7.941161228	3.475737668	4.46542356	IED
7	BrMOB	EVE	7.920480412	3.481179988	4.43930042	IED
8	IMOB	EVE	8.146880924	3.141307104	5.00557382	IED

rich dienophile EVE were selected for theoretical studies. In the Diels–Alder reaction of MOBs, there are four possible reaction pathways based on the approach of the R group (Ac of MVK or OEt of EVE) with respect to the carbonyl group of MOB, *viz.* *ortho*/*endo*, *ortho*/*exo*, *meta*/*endo* and *meta*/*exo* (Fig. 1). We denote the corresponding transition state structures as **TS1$_{ON}$**, **TS1$_{OX}$**, **TS1$_{MN}$** and **TS1$_{MX}$** (of reactions with MVK) and **TS2$_{ON}$**, **TS2$_{OX}$**, **TS2$_{MN}$** and **TS2$_{MX}$** (of reactions with EVE), where **ON**, **OX**, **MN** & **MX** related to *ortho–endo*, *ortho–exo*, *meta–endo* & *meta–exo*, respectively. From these TSs, the related minima associated with the final products are **P1$_{ON}$**, **P1$_{OX}$**, **P1$_{MN}$** & **P1$_{MX}$** (from MVK) and **P2$_{ON}$**, **P2$_{OX}$**, **P2$_{MN}$** & **P2$_{MX}$** (from EVE), respectively.

The selected geometric parameters of the calculated TSs are shown in Fig. 2, and Table 7 presents the calculated values of transition state energies and relative energies for stationary points. The table also includes information on the distance between bond-forming atoms in dienes and dienophiles in each case. A schematic representation of the different reaction pathways for each of the reactions (a) Br-MOB + MVK and (b) Br-MOB + EVE is depicted in Fig. 3. As can be seen from Table 7, the theory is successful in its predictions. For the cycloaddition reactions of halo MOBs with MA, the theory correctly predicts that *ortho* approaches are with minimum potential energy barrier (PEB) and *ortho–endo* adducts are the preferred products. The transition states **TS1$_{ON}$-F**, **TS1$_{ON}$-Cl**, **TS1$_{ON}$-Br** & **TS1$_{ON}$-I** of *ortho–endo* adducts are stable over transition states **TS1$_{OX}$-F, TS1$_{OX}$-Cl, TS1$_{OX}$-Br & TS1$_{OX}$-I** of *ortho–exo* adducts by a large amount of 4.05, 3.19, 3.27 and 4.03 kcal mol^{-1}, respectively. The PEBs of *ortho* approaches in the reaction of halo MOBs and EVE are again preferred over the *meta* approaches. However, the energy barrier between **TS2$_{ON}$** and **TS2$_{OX}$** is less. The *ortho–exo* approaches **TS2$_{OX}$-Cl and TS2$_{OX}$-I** are slightly favoured over their *ortho–endo* approaches, which is against the experimental outcome. The preference of **TS2$_{ON}$-I** was regained from **TS2$_{OX}$-I** when the calculations were performed in methanolic medium.

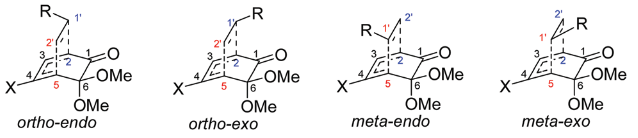

Fig. 1 The four possible transition states for the reaction between an MOB and a dienophile.

The Diels–Alder reactions of MOBs are unique in delivering the cycloadducts in a highly stereo- and regio-selective manner. In these cycloadditions, the initial bond formation occurs at C-5 of MOB.[3b,28,29] Even in the reactions of halo MOBs, the same trend was observed. Among the two σ-bonds C_5–$C_{2'}$ and C_2–$C_{1'}$ being formed, the distance between C_5 of MOB and $C_{2'}$ of the dienophile is less than that of C_2 of MOB and $C_{1'}$ of the dienophile indicating that the initial bond is being formed at C_5 of MOB. Despite the large asynchronicity (ranging from 2.92 to 3.58 for MVK reactions and from 3.18 to 3.67 for EVE reactions) for the *ortho* regioisomers, the cycloaddition takes place *via* an asynchronous process, in which the C-5–C-2′ bond is being formed first, while the C2 and C1′ atoms are not yet being bonded at the TS. On the other hand, the non-expected *meta* pathway proceeds *via* a concerted process, where the two σ-bonds are formed simultaneously, but dissymmetrically.

The *endo* preference is generally explained by invoking secondary orbital interactions (SOI) even for dienophiles bearing electron-releasing substituents. The geometries of the *ortho–endo* TSs displayed distances in the range of 2.92–3.11 Å between C-3/C-4 of MOBs and C═O group of MVK and 3.19–3.40 Å with the oxygen atom of EVE. These distances may be sufficient to invoke SOI. Alternatively, the large *ortho–endo* preference may be attributed to the existence of a destabilizing interaction[31] in *meta–endo* and *meta–exo* transition states that arises from electrostatic and/or van der Waals interactions between the R group (*e.g.*, Ac of MVK and OEt of EVE) of the dienophile and the halo substituent/methoxy group of the ketal function owing to their close proximity. The *ortho–exo* TS also experiences such interactions but to a lesser extent as evidenced from its lower PEB in comparison with those of *meta* TSs. To obtain better insights into non-stereoselective Diels–Alder reactions of MOBs with acrylonitrile and vinyl acetate, we have studied the quantum mechanical calculations for the reactions between (i) 4-chloro MOB and ACN and (ii) 4-chloro MOB and VA to obtain the PEBs of different approaches in the transition state. The data (see Table S-16 of ESI†) suggested that in both cases, the *endo* approach is less energetic and the *ortho–endo*, *ortho–exo* TSs have comparable energies (15.25 & 15.86 kcal mol^{-1} and 21.80 & 21.19 kcal mol^{-1} for the reactions of ACN and VA, respectively). Thus the theoretical data support the formation of *ortho–endo* and *ortho–exo* products that are observed experimentally from the

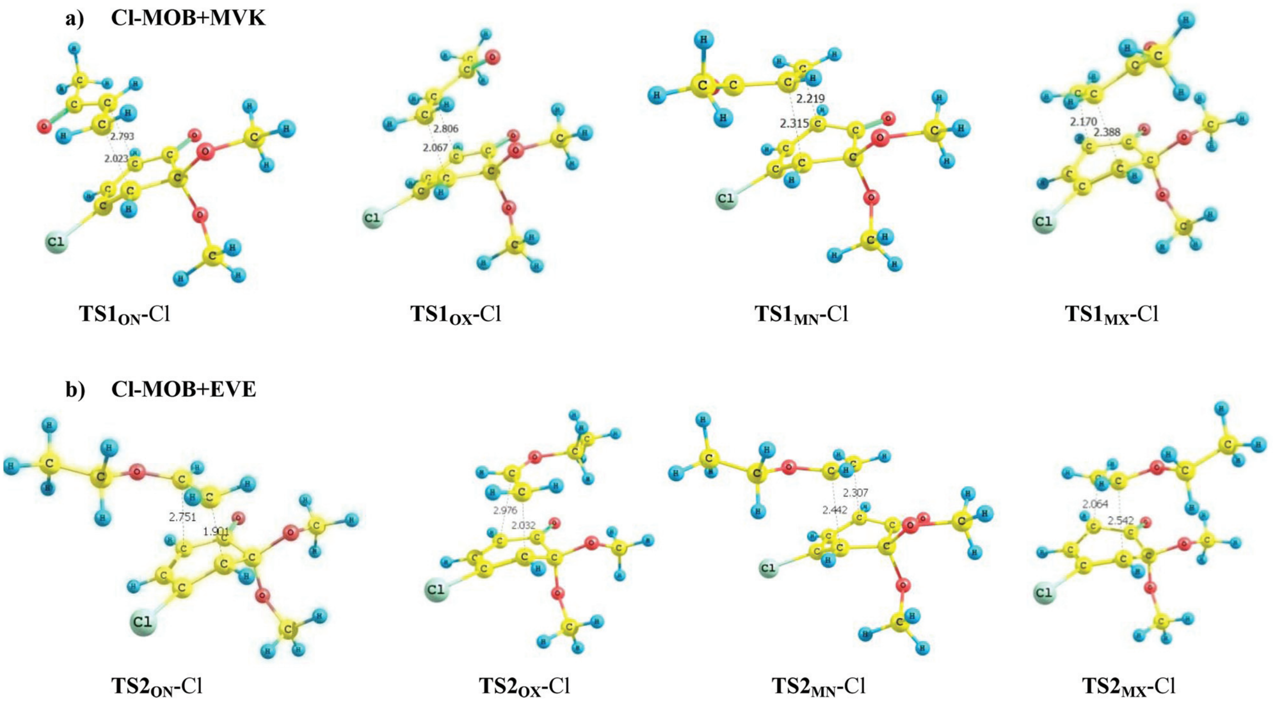

Fig. 2 Optimized geometries for the transition states of reactions between chloro MOB and (a) MVK and (b) EVE.

Table 7 Total energies (in au) and relative energies (in kcal mol^{-1}) for the transition states corresponding to the cycloaddition reaction between halo MOBs and MVK/EVE

		Cycloaddition with MVK				Cycloaddition with EVE			
4-Halo MOB	Config.	B3LYP/6-31G**	Rel ene (kcal mol^{-1})	C_5–$C_{n'}$ (Å)	C_2–$C_{n'}$ (Å)	B3LYP/6-31G**	Rel ene (kcal mol^{-1})	C_5–$C_{n'}$ (Å)	C_2–$C_{n'}$ (Å)
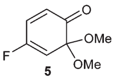 **5**	*ortho–endo*	−866.9401133	11.93	1.91888	2.78550	−868.1290825	19.27	1.94055	2.78403
	ortho–exo	−866.9336468	15.98	2.03426	2.74058	−868.1290204	19.31	1.99628	2.87542
	meta–endo	−866.9323442	16.80	2.35963	2.23286	−868.128417	19.69	2.41458	2.29710
	meta–exo	−866.9251091	21.34	2.43103	2.17443	−868.1199958	24.97	2.57943	2.03486
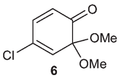 **6**	*ortho–endo*	−1227.3019549	12.24	2.02331	2.79346	−1228.4946613	17.24	1.90104	2.75090
	ortho–exo	−1227.2968698	15.43	2.06667	2.80647	−1228.495579	16.66	2.03186	2.97621
	meta–endo	−1227.2942833	17.05	2.31512	2.21854	−1228.4905152	19.84	2.44226	2.30749
	meta–exo	−1227.2889173	20.42	2.38832	2.17023	−1228.4837049	24.11	2.54196	2.06447
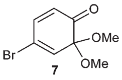 **7**	*ortho–endo*	−3338.812108	11.48	2.01599	2.82903	−3340.0073707	14.88	1.95316	2.88237
	ortho–exo	−3338.8069004	14.75	2.02861	2.74718	−3340.0061677	15.63	2.00415	2.93764
	meta–endo	−3338.8054029	15.69	2.31229	2.21997	−3340.0021762	18.14	2.33821	2.22190
	meta–exo	−3338.7988166	19.82	2.39481	2.18982	−3339.9933393	23.68	2.51228	2.08551
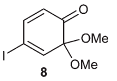 **8**	*ortho–endo*	−7687.0411318	0.99	2.03928	2.80180	−7688.2332563	6.35	1.97379	2.90106
	ortho–exo	−7687.034717	5.02	2.25001	3.00372	−7688.2334107	6.26	1.77610	2.76643
	meta–endo	−7687.0332597	5.93	2.28616	2.17562	−7688.2282164	9.52	2.23009	2.08860
	meta–exo	−7687.0276703	9.44	2.31084	2.07949	−7688.2218882	13.49	2.44381	1.88664

reactions between 4-halo-MOBs and acrylonitrile and vinyl acetate.

Global electronic indexes – electronic chemical potential μ, chemical hardness η and electrophilicity ω – are useful tools for understanding the reactivity of molecules in their ground state.[32] The larger electronic chemical potential of dienophiles (μ = −0.0893 to −0.1511 au) in comparison with that of MOBs (μ = −0.1683 to −0.1813 au) indicates that the net charge transfer is taking place from dienophiles to MOB, which is also supportive of the inverse electron-demand Diels–Alder reaction (Table 8). The large electrophilicity power of MOBs (ω = 2.54 to 3.06 eV) and the low electrophilicity power of dienophiles (ω = 0.40 to 1.61 eV) indicate the electrophilic nature of MOBs and the nucleophilic nature of dienophiles. The data obtained from the condensed Fukui functions suggest that the carbon C-5 of MOBs **6–8** has the largest electrophilic activation (f_k^+ = 0.14–0.19) in comparison with carbon C-2 (f_k^+ = 0.13–0.15) and the highest nucleophilic Fukui function of EVE is on C-2′ (f_k^- = 0.27) in comparison with C-1′ (f_k^- = 0.10). This supports the formation of the *ortho* product as observed experimentally. The nucleophilic Fukui functions on the electron-deficient dienophile MVK do not support the experimental observation.

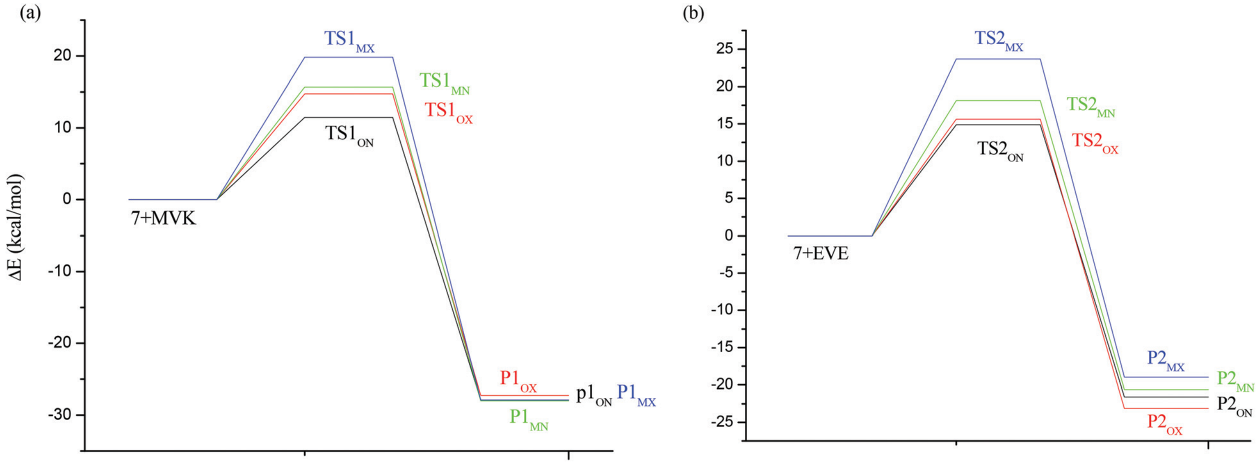

Fig. 3 Schematic representation of the different energy profiles for the reaction between (a) Br-MOB (**7**) and methyl vinyl ketone (MVK), (b) Br-MOB (**7**) and ethyl vinyl ether (EVE).

Table 8 Global properties of MOBs **5–8** and dienophiles MVK and EVE

Reactant	μ (a.u.)	η (a.u.)	ω (eV)
F MOB (**5**)	−0.16831	0.15171	2.540542
Cl MOB (**6**)	−0.17135	0.15088	2.647630
Br MOB (**7**)	−0.17087	0.15032	2.642626
I MOB (**8**)	−0.18128	0.14615	3.059298
MVK	−0.15108	0.19259	1.612505
EVE	−0.08930	0.26868	0.403821

Conclusion

We have demonstrated that the title 4-halo-orthobenzoquinone monoketals (X = F, Cl, I) are stable enough for the isolation and characterization. A practical chemical protocol for the synthesis of highly substituted bicyclo[2.2.2]octenone derivatives in a highly regio- and stereo-selective manner from the corresponding 4-haloguaiacols is now available. The assigned regio- and stereo-selectivities are confirmed by NMR analysis including 1D and 2D NMR experiments and single crystal X-ray analysis.

These reactions can be classified as inverse electron-demand Diels–Alder reactions since the difference in energy gaps ($\Delta\Delta E$) between two possible interactions is about 1 eV (with MVK) and about 4.5 eV (with EVE). These results indicate that the 4-halo MOBs undergo inverse electron-demand Diels–Alder reactions with two different types of dienophiles.

The computed energies of transition state structures are successful in predicting *regio*- and *stereo*-selectivity. For the reactions of halo MOBs with EVE, the theory correctly predicts that *ortho* approaches are with minimum potential energy barrier and *ortho–endo* adducts are the preferred products. The PEBs of *ortho* approaches in the reaction of halo MOBs and EVE are again preferred over the *meta* approaches. Analogous to MOB Diels–Alder chemistry, the initial bond formation occurs at C-5 of halo MOBs in the current addition reactions. The cycloaddition proceeds *via* an asynchronous process, in which the C-5–C-2′ bond is formed first, while the C-2 and C-1′ atoms are not yet bonded at the TS.

While the Fukui indices suggested the *ortho* regiochemistry of adducts from EVE, which is in line with the experimental observation, the nucleophilic Fukui functions on the electron-deficient dienophile MVK do not support the *ortho* selectivity.

Experimental section

General

All reagents were purchased at the highest commercially quality and used without further purification. Solvents were purified by standard methods. Yields refer to chromatographically homogeneous materials, unless otherwise stated. Reactions were monitored by thin-layer chromatography (TLC) carried out on 0.25 mm silica gel plates (60F-254) using UV light as a visualizer or in an iodine chamber. Silica gel (particle size 100–200 mesh) was used for column chromatography with ethyl acetate–hexanes as an eluent system. Melting points are uncorrected.

Instrumentation

IR spectra of the compounds are expressed as wavenumbers (cm^{-1}). NMR spectra were recorded in $CDCl_3$ using TMS as an internal standard. Chemical shifts of ^1H NMR spectra were given in parts per million with respect to TMS and the coupling constant *J* was measured in Hz. The signals from the solvent $CDCl_3$, 7.26 (residual $CHCl_3$) and 77.0 ppm, are set as the reference peaks in ^1H NMR and ^{13}C NMR spectra, respectively. The following abbreviations were used to explain the multiplicities: s = singlet, d = doublet, t = triplet, q = quartet, m = multiplet, b = broad, dd = doublet of doublet, ddd = doublet of doublet of doublet, dt = doublet of triplet, qd = quartet of doublet. Mass spectra were recorded by the electrospray ionization method using a quadrupole analyzer.

Generation of MOBs. To a solution of 4-halo-2-methoxyphenol (1 mmol) in anhydrous methanol (4 mL) was added a solution of DAIB (0.354 mg, 1.1 mmol) in anhydrous methanol (6 mL) over a period of 10 min at 0 °C under a nitrogen atmosphere. After 10 min, the ice bath was removed. After the reaction was complete, the reaction mixture was concentrated using a rotary evaporator under reduced pressure and the residue was purified by silica gel column flash chromatography with 10% ethyl acetate in hexanes as an eluent to furnish the pure 4-halo masked *o*-benzoquinone.

6,6-Dimethoxy-4-fluorocyclohexa-2,4-dienone (5a). Yield 0.154 g (89%) as a yellowish liquid; IR (KBr) $\nu_{\max}$ 1740, 1646, 1232, 1201, 1105 cm^{-1}; ^{1}H NMR (500 MHz, CDCl$_3$) δ 6.81 (ddd, *J* = 3.0, 6.5, 10.0 Hz, 1H), 6.08 (dd, *J* = 6.0, 10.5 Hz, 1H), 5.91 (dd, *J* = 3.0, 11.0 Hz, 1H), 3.36 (s, 6H) ppm; ^{13}C NMR (125 MHz, CDCl$_3$) δ 193.1 (C=O), 158.2 & 156.2 (C-4), 135.9 & 135.6 (C-5), 127.5 & 127.4 (C-3), 110.2 & 110.1 (C-2), 92.9 & 92.7 (C-6), 50.1 (OMe) ppm.

4-Chloro-6,6-dimethoxycyclohexa-2,4-dienone (6a). Yield 0.166 g (88%) as a yellowish liquid; IR (KBr) $\nu_{\max}$ 1744, 1691, 1632, 1268, 1108, 1054, 1029 cm^{-1}; ^{1}H NMR (500 MHz, CDCl$_3$) δ 6.78 (dd, *J* = 2.5, 10.5 Hz, 1H), 6.44 (d, *J* = 2.5 Hz, 1H), 6.05 (d, *J* = 10.5 Hz, 1H), 3.37 (s, 6H) ppm; ^{13}C NMR (125 MHz, CDCl$_3$) δ 192.9 (C=O), 141.4 (C-5), 131.1 (C-4), 130.8 (C-3), 126.6 (C-2), 92.2 (C-6), 50.2 (OMe) ppm.

6,6-Dimethoxy-4-iodocyclohexa-2,4-dienone (8a). Yield 0.246 g (88%) as a yellowish liquid; IR (KBr) $\nu_{\max}$ 1743, 1687, 1615, 1252, 1139, 1061 cm^{-1}; ^{1}H NMR (500 MHz, CDCl$_3$) δ 6.99–6.96 (m, 2H), 5.80 (d, *J* = 9.5 Hz, 1H), 3.37 (s, 6H) ppm. ^{13}C NMR (125 MHz, CDCl$_3$) δ 192.8 (C=O), 147.0 (C-5), 143.9 (C-3), 126.4 (C-2), 93.3 (C-6), 91.1 (C-4), 50.3 (OMe) ppm.

Method A: To a solution of 4-halo-2-methoxyphenol (1 mmol) and a dienophile (25 mmol) in anhydrous methanol (4 mL) was added a solution of DAIB (0.354 mg, 1.1 mmol) in anhydrous methanol (6 mL) over a period of 30 min at 0 °C under a nitrogen atmosphere. After 10 min, the ice bath was removed and the contents were allowed to stir at room temperature for the time specified in Table 1. After the reaction was complete, the reaction mixture was concentrated using a rotary evaporator under reduced pressure and the residue was purified by silica gel column chromatography with 10% ethyl acetate in hexanes as an eluent to furnish the cycloadduct.

Method B: To a solution of 4-halo-2-methoxyphenol (1 mmol) and a dienophile (25 mmol) in anhydrous methanol (4 mL) was added a solution of DAIB (0.354 mg, 1.1 mmol) in anhydrous methanol (6 mL) over a period of 1 h at 50 °C under a nitrogen atmosphere. Stirring was continued for another 1 h at the same temperature for the reaction to reach completion. The products were purified in a similar manner as mentioned in Method A.

(1*S,4*R**,7*S**)-3,3-Dimethoxy-5-fluoro-7-methoxycarbonylbicyclo[2.2.2]oct-5-en-2-one (9a).** Yield 0.186 g (72%) as a viscous liquid; IR (KBr) $\nu_{\max}$ 1739, 1670, 1448, 1361, 1205, 1163, 1073 cm^{-1}; ^{1}H NMR (500 MHz, CDCl$_3$) δ 5.35–5.31 (m, 1H), 3.71 (s, 3H), 3.52 (ddd, *J* = 2.0, 4.0, 6.5 Hz, 1H), 3.38 (s, 3H), 3.34 (s, 3H), 3.17 (qd, *J* = 3.0, 6.0 Hz, 1H), 3.02–3.00 (m, 1H), 2.29 (ddd, *J* = 2.5, 10.0, 13.5 Hz, 1H), 2.11 (ddd, *J* = 3.0, 5.5, 13.5 Hz, 1H) ppm; ^{13}C NMR (125 MHz, CDCl$_3$) δ 199.6, 172.6, 165.1 & 162.8 (C-5), 97.1 & 97.0 (C-6), 93.6, 52.3, 50.5, 49.9, 48.2 & 48.1 (C-1), 41.6 & 41.4 (C-4), 39.1, 24.2 ppm; HRMS (ESI+) calcd for $C_{12}H_{15}FO_5Na$ $[M + Na]^+$: 281.0801. Found: 281.0807.

(1*S,4*R**,7*S**)-3,3-Dimethoxy-5-fluoro-7-methoxycarbonyl-7-methylbicyclo[2.2.2]oct-5-en-2-one (9b).** Yield 0.166 g (61%) as a viscous liquid; IR (KBr) $\nu_{\max}$ 1736, 1673, 1455, 1367, 1292, 1120 cm^{-1}; ^{1}H NMR (500 MHz, CDCl$_3$) δ 5.36–5.33 (m, 1H), 3.70 (s, 3H), 3.38 (s, 3H), 3.36 (s, 3H), 3.34 (dd, *J* = 4.0, 7.0 Hz, 1H), 3.09 (dd, *J* = 2.5, 14.0 Hz, 1H), 2.61 (dd, *J* = 3.5, 14.0 Hz, 1H), 1.84 (dd, *J* = 3.0, 14.0 Hz, 1H), 1.31 (s, 3H) ppm; ^{13}C NMR (125 MHz, CDCl$_3$) δ 200.8, 175.7, 165.4 & 163.2 (C-5), 98.9 & 98.8 (C-6), 93.9, 54.5 & 54.4 (C-1), 52.3, 50.6, 49.7, 46.8, 41.6 & 41.5 (C-4), 30.6, 25.2 ppm; HRMS (ESI+) calcd for $C_{13}H_{17}FO_5Na$ $[M + Na]^+$: 295.0958. Found: 295.0956.

(1*S,4*R**,7*S**)-7-Acetyl-3,3-dimethoxy-5-fluorobicyclo[2.2.2]-oct-5-en-2-one (9c).** Yield 0.222 g (91%) as a viscous liquid; IR (KBr) $\nu_{\max}$ 1741, 1671, 1364, 1162, 1129, 1090, 1067 cm^{-1}; ^{1}H NMR (500 MHz, CDCl$_3$) δ 5.28 (ddd, *J* = 2.5, 5.0, 7.5 Hz, 1H), 3.46 (ddd, *J* = 2.0, 4.0, 7.0 Hz, 1H), 3.38 (s, 3H), 3.35 (s, 3H), 3.18 (qd, *J* = 3.0, 14.0 Hz, 1H), 3.04–3.01 (m, 1H), 2.22 (ddd, *J* = 2.5, 10.0, 13.5 Hz, 1H), 2.19 (s, 3H), 2.06 (ddd, *J* = 3.0, 6.0, 13.5 Hz, 1H) ppm; ^{13}C NMR (125 MHz, CDCl$_3$) δ 205.0, 199.8, 164.8 & 162.5 (C-5), 96.8 & 96.7 (C-6), 93.8, 50.7, 50.0, 47.8 & 47.7 (C-1), 47.0, 41.6 & 41.5 (C-4), 28.2, 23.1 ppm; HRMS (ESI+) calcd for $C_{12}H_{15}FO_4Na$ $[M + Na]^+$: 265.0852. Found: 265.0848.

(1*S,2*RS*,4*R**)-5-Fluoro-8,8-dimethoxy-7-oxobicyclo[2.2.2]oct-5-en-2-yl cyanide (9d).** Yield 0.135 g (60%) as a viscous liquid; IR (KBr) $\nu_{\max}$ 2927, 1623 cm^{-1}; ^{1}H NMR (500 MHz, CDCl$_3$) δ 5.54 (sept, *J* = 7.0 Hz, 1H), 5.40 (sept, *J* = 3.0 Hz, 1H), 3.86 (s, 3H), 3.76 (s, 3H), 3.44–3.43 (m, 1H), 3.40 (s, 2H), 3.38 (s, 1H), 3.37 (s, 4H), 3.32 (s, 4H), 3.26–3.22 (m, 2H), 3.16–3.14 (m, 1H), 2.92 (ddd, *J* = 3.5, 6.5, 12.0 Hz, 1H), 2.55–2.44 (m, 2H), 2.17 (ddd, *J* = 2.5, 7.5, 13.5 Hz, 1H), 1.97 (ddd, *J* = 4.0, 7.5, 13.5 Hz, 1H) ppm.

(1*S,4*R**,7*S**)-5-Chloro-3,3-dimethoxy-7-methoxycarbonylbicyclo[2.2.2]oct-5-en-2-one (10a).** Yield 0.252 g (92%) as a viscous liquid; IR (KBr) $\nu_{\max}$ 2952, 1734, 1623, 1446, 1325, 1298, 1206, 1104 cm^{-1}; ^{1}H NMR (500 MHz, CDCl$_3$) δ 6.05 (dd, *J* = 2.5, 7.0 Hz, 1H), 3.71 (s, 3H), 3.57 (dd, *J* = 2.0, 7.0 Hz, 1H), 3.39 (s, 3H), 3.35 (s, 3H), 3.24 (q, *J* = 2.0 Hz, 1H), 3.04 (ddd, *J* = 2.0, 6.0, 10.0 Hz, 1H), 2.34 (ddd, *J* = 3.0, 10.5, 13.5 Hz, 1H), 2.02 (ddd, *J* = 3.0, 5.5, 13.5 Hz, 1H) ppm; ^{13}C NMR (125 MHz, CDCl$_3$) δ 199.2, 172.6, 137.1, 120.4, 93.5, 52.4, 50.8, 50.7, 50.1, 47.4, 39.0, 24.7 ppm; HRMS (ESI+) calcd for $C_{12}H_{15}ClO_5Na$ $[M + Na]^+$: 297.0500. Found: 297.0496.

(1*S,4*R**,7*S**)-5-Chloro-3,3-dimethoxy-7-methoxycarbonyl-7-methylbicyclo[2.2.2]oct-5-en-2-one (10b).** Yield 0.208 g (72%) as a white solid: mp 58–60 °C; IR (KBr) $\nu_{\max}$ 2964, 1737, 1623, 1456, 1378, 1291, 1120 cm^{-1}; ^{1}H NMR (500 MHz, CDCl$_3$) δ 6.07 (dd, *J* = 2.5, 7.0 Hz, 1H), 3.70 (s, 3H), 3.40 (d, *J* = 6.5 Hz, 1H), 3.39 (s, 3H), 3.37 (s, 3H), 3.17 (q, *J* = 2.5 Hz, 1H), 2.52 (dd, *J* = 3.5, 13.5 Hz, 1H), 1.90 (dd, *J* = 2.5, 14.0 Hz, 1H), 1.31 (s, 3H) ppm;

^{13}C NMR (125 MHz, CDCl$_3$) δ 200.4, 175.7, 137.1, 122.2, 93.7, 57.2, 52.6, 50.7, 49.8, 47.6, 46.7, 31.9, 25.3 ppm; HRMS (ESI+) calcd for $C_{13}H_{17}ClO_5Na$ [M + Na]$^+$: 311.0662. Found: 311.0655.

(1*S,4*R**,7*S**)-7-Acetyl-5-chloro-3,3-dimethoxybicyclo[2.2.2]-oct-5-en-2-one (10c).** Yield 0.202 g (78%) as a viscous liquid; IR (KBr) ν_{max} 1741, 1625, 1362, 1131, 1101, 1062 cm^{-1}; ^{1}H NMR (500 MHz, CDCl$_3$) δ 6.02 (dd, *J* = 2.0, 6.5 Hz, 1H), 3.50 (dd, *J* = 2.0, 7.0 Hz, 1H), 3.39 (s, 3H), 3.36 (s, 3H), 3.25 (q, *J* = 2.5 Hz, 1H), 3.07 (ddd, *J* = 1.5, 6.5, 10.0 Hz, 1H), 2.30 (ddd, *J* = 3.0, 10.0, 13.0 Hz, 1H), 2.18 (s, 3H), 1.92 (ddd, *J* = 2.5, 6.0, 13.0 Hz, 1H) ppm; ^{13}C NMR (125 MHz, CDCl$_3$) δ 204.9, 199.4, 136.2, 120.4, 93.6, 50.6, 50.3, 50.1, 47.4, 46.9, 28.2, 23.7 ppm; HRMS (ESI+) calcd for $C_{12}H_{15}ClO_4Na$ [M + Na]$^+$: 281.0557. Found: 281.0552.

(1*S,2*RS*,4*R**)-5-Chloro-8,8-dimethoxy-7-oxobicyclo[2.2.2]oct-5-en-2-yl cyanide (10d).** Yield 0.193 g (80%) as a viscous liquid; IR (KBr) ν_{max} 2360, 1768 cm^{-1}; ^{1}H NMR (500 MHz, CDCl$_3$) δ 6.22 (dd, *J* = 2.5, 6.5 Hz, 1H), 6.10 (dd, *J* = 4.5, 6.5 Hz, 1H), 3.60 (s, 6H), 3.48 (dd, *J* = 2.0, 7.0 Hz, 1H), 3.47–3.39 (m, 1H), 3.38 (s, 3H), 3.33 (s, 3H), 3.31–3.19 (m, 2H), 3.17 (ddd, *J* = 2.0, 5.5, 10.0 Hz, 1H), 2.95–2.93 (m, 1H), 2.54 (ddd, *J* = 2.5, 10.0, 13.0 1H), 2.49–2.44 (m, 1H), 1.96–1.92 (m, 1H), 1.93 (ddd, *J* = 3.0, 5.5, 13.5 Hz, 1H) ppm.

(1*S,4*R**,7*S**)-3,3-Dimethoxy-5-iodo-7-methoxycarbonyl-bicyclo[2.2.2]oct-5-en-2-one (11a).** Yield 0.354 g (97%) as a yellowish liquid; IR (KBr) ν_{max} 1739, 1638, 1436, 1197, 1097, 1063 cm^{-1}; ^{1}H NMR (500 MHz, CDCl$_3$) δ 6.60 (dd, *J* = 2.5, 7.0 Hz, 1H), 3.71 (s, 3H), 3.45 (dd, *J* = 2.0, 7.0 Hz, 1H), 3.39 (s, 3H), 3.37 (q, *J* = 2.5 Hz, 1H), 3.33 (s, 3H), 3.02 (ddd, *J* = 1.5, 6.0, 9.5 Hz, 1H), 2.26 (ddd, *J* = 3.0, 10.0, 13.0 Hz, 1H), 1.95 (ddd, *J* = 2.5, 6.0, 13.0 Hz, 1H) ppm; ^{13}C NMR (125 MHz, CDCl$_3$) δ 198.7, 172.7, 133.9, 95.8, 93.9, 53.3, 52.4, 52.0, 51.0, 50.1, 38.7, 24.8 ppm; HRMS (ESI+) calcd for $C_{12}H_{15}IO_5Na$ [M + Na]$^+$: 388.9856. Found: 388.9854.

(1*S,4*R**,7*S**)-3,3-Dimethoxy-5-iodo-7-methoxycarbonyl-7-methylbicyclo[2.2.2]oct-5-en-2-one (11b).** Yield 0.342 g (90%) as a yellow solid: mp 88–89 °C; IR (KBr) ν_{max} 1737, 1638, 1442, 1382, 1215, 1125, 1049 cm^{-1}; ^{1}H NMR (500 MHz, CDCl$_3$) δ 6.63 (dd, *J* = 2.0, 7.0 Hz, 1H), 3.70 (s, 3H), 3.39 (s, 3H), 3.35 (s, 3H), 3.30 (d, *J* = 6.5 Hz, 2H), 2.45 (dd, *J* = 3.5, 13.5 Hz, 1H), 1.84 (dd, *J* = 3.0, 14.0 Hz, 1H), 1.29 (s, 3H) ppm; ^{13}C NMR (125 MHz, CDCl$_3$) δ 200.0, 175.6, 135.8, 95.7, 94.1, 59.8, 52.6, 52.2, 51.0, 49.8, 46.3, 32.0, 25.2 ppm. HRMS (ESI+) calcd for $C_{13}H_{17}IO_5Na$ [M + Na]$^+$: 403.0018. Found: 403.0023.

(1*S,4*R**,7*S**)-7-Acetyl-3,3-dimethoxy-5-iodobicyclo[2.2.2]oct-5-en-2-one (11c).** Yield 0.298 g (85%) as a white solid: mp 74–76 °C; IR (KBr) ν_{max} 1738, 1642, 1457, 1364, 1267, 1135, 1067 cm^{-1}; ^{1}H NMR (500 MHz, CDCl$_3$) δ 6.58 (dd, *J* = 2.0, 7.0 Hz, 1H), 3.41–3.40 (m, 1H), 3.39 (s, 3H), 3.38–3.37 (m, 1H), 3.35 (s, 3H), 3.05 (ddd, *J* = 1.0, 6.5, 9.5 Hz, 1H), 2.24 (ddd, *J* = 3.0, 10.0, 13.0 Hz, 1H), 2.17 (s, 3H), 1.84 (ddd, *J* = 2.5, 6.0, 13.0 Hz, 1H) ppm; ^{13}C NMR (125 MHz, CDCl$_3$) δ 205.0, 199.1, 134.1, 94.8, 94.2, 52.8, 52.1, 51.0, 50.2, 46.8, 28.2, 24.0 ppm; HRMS (ESI+) calcd for $C_{12}H_{15}IO_4Na$ [M + Na]$^+$: 372.9913. Found: 372.9906.

(1*S,2*RS*,4*R**)-5-Iodo-8,8-dimethoxy-7-oxobicyclo[2.2.2]oct-5-en-2-yl cyanide (11d).** (All the data given here belong to the mixture of *endo* and *exo*.) Yield 0.310 g (93%) as a viscous liquid; IR (KBr) ν_{max} 2935, 2240, 1737 cm^{-1}; ^{1}H NMR (500 MHz, CDCl$_3$) δ 6.77 (dd, *J* = 2.0, 7.0 Hz, 1H), 6.64 (dd, *J* = 2.0, 7.0 Hz, 1H), 3.45–3.43 (m, 1H), 3.43–3.41 (m, 1H), 3.40 (s, 3H), 3.39 (s, 3H), 3.38 (s, 3H), 3.37–3.32 (m, 2H), 3.31 (s, 3H), 3.16 (ddd, *J* = 1.5, 5.5, 9.5 Hz, 1H), 2.92 (ddd, *J* = 3.5, 7.5, 14.0 Hz, 1H), 2.45 (ddd, *J* = 3.0, 10.0, 13.0 Hz, 1H), 2.36 (ddd, *J* = 3.0, 10.0, 13.0 Hz, 1H), 2.07 (ddd, *J* = 2.5, 6.0, 13.5 Hz, 1H), 1.88 (ddd, *J* = 3.0, 6.0, 13.5 Hz, 1H) ppm.

General procedure for Diels–Alder reaction between 4-halo MOBs and electron-rich dienophiles. To a solution of 4-halo-2-methoxyphenol (0.5 mmol) in anhydrous methanol (5 mL) was added DAIB (0.193 mg, 0.6 mmol) at 0 °C under a nitrogen atmosphere. After 10 min of stirring, a dienophile (10 mmol) was added at the same temperature. Then the temperature was allowed to rise to RT and stirring was continued until complete disappearance of MOB (the time specified in Table 2). After the reaction was complete, the reaction mixture was concentrated using a rotary evaporator under reduced pressure and the residue was purified by silica gel column chromatography with 10% ethyl acetate in hexanes as an eluent to furnish the cycloadduct.

(1*S,4*R**,7*S**)-3,3-Dimethoxy-5-fluoro-7-phenylbicyclo[2.2.2]-oct-5-en-2-one (12a).** Yield 0.088 g (65%) as a white solid: mp 71–73 °C; IR (KBr) ν_{max} 1740, 1673, 1454, 1363, 1170, 1066 cm^{-1}; ^{1}H NMR (500 MHz, CDCl$_3$) δ 7.31–7.28 (m, 2H), 7.25–7.22 (m, 1H), 7.21–7.19 (m, 2H), 5.32 (ddd, *J* = 3.0, 5.5, 10.0 Hz, 1H), 3.42 (s, 3H), 3.40 (s, 3H), 3.38–3.35 (m, 1H), 3.26 (qd, *J* = 3.0, 5.5 Hz, 1H), 3.21 (ddd, *J* = 2.0, 4.5, 7.0 Hz, 1H), 2.57 (ddd, *J* = 2.5, 10.5, 14.0 Hz, 1H), 1.89 (ddd, *J* = 3.0, 7.5, 13.5 Hz, 1H) ppm; ^{13}C NMR (125 MHz, CDCl$_3$) δ 200.5, 165.2 & 163.0 (C-5), 143.2, 128.7, 127.7, 127.0, 96.9, 93.6, 53.1, 50.7, 50.1, 42.4 & 42.2 (C-4), 39.7, 30.1 ppm; HRMS (ESI+) calcd for $C_{16}H_{17}FO_3Na$ [M + Na]$^+$: 299.1059. Found: 299.1069.

(1*S,4*R**,7*S**)-5-Chloro-3,3-dimethoxy-7-phenylbicyclo[2.2.2]-oct-5-en-2-one (13a).** Yield 0.130 g (89%) as a white solid: mp 71–72 °C; IR (KBr) ν_{max} 1737, 1611, 1490, 1455, 1326, 1199, 1136, 1098, 1064 cm^{-1}; ^{1}H NMR (500 MHz, CDCl$_3$) δ 7.31–7.21 (m, 3H), 7.16–7.14 (m, 2H), 6.04 (dd, *J* = 2.5, 6.5 Hz, 1H), 3.42 (s, 3H), 3.41 (s, 3H), 3.40–3.38 (m, 1H), 3.33–3.31 (m, 1H), 3.27 (dd, *J* = 2.0, 7.0 Hz, 1H), 2.58 (ddd, *J* = 3.0, 9.5, 13.0 Hz, 1H), 1.85 (ddd, *J* = 2.5, 6.5, 13.5 Hz, 1H) ppm; ^{13}C NMR (125 MHz, CDCl$_3$) δ 200.3, 143.2, 136.8, 128.8, 127.6, 127.1, 120.4, 93.6, 56.1, 50.8, 50.3, 48.3, 40.1, 30.2 ppm; HRMS (ESI+) calcd for $C_{16}H_{17}ClO_3Na$ [M + Na]$^+$ and [M + 2 + Na]$^+$: 315.0763 and 317.0734. Found: 315.0769 and 317.0738.

(1*R,2*R**,6*R**,7*R**)-11-Chloro-8,8-dimethoxy-3-oxatricyclo-[5.2.2.0^{2,6}]undec-10-en-9-one (13b).** Yield 0.134 g (90%) as a brown viscous liquid; IR (KBr) ν_{max} 1740, 1598, 1498, 1452, 1351, 1271, 1224, 1097, 1043 cm^{-1}; ^{1}H NMR (500 MHz, CDCl$_3$) δ 6.03–6.01 (m, 1H), 4.33 (dd, *J* = 3.0, 8.0 Hz, 1H), 3.95 (dt, *J* = 3.0, 8.0 Hz, 1H), 3.62–3.57 (m, 2H), 3.38 (s, 3H), 3.35 (s, 3H), 3.27 (apparent t, *J* = 2.5, 1H), 3.00 (dq, *J* = 3.0, 8.5 Hz, 1H), 2.15 (dddd, *J* = 3.0, 6.5, 9.5, 12.5 Hz, 1H), 1.76–1.68 (m, 1H) ppm; ^{13}C NMR (125 MHz, CDCl$_3$) δ 199.5, 134.6, 120.8, 93.0, 78.1, 69.1, 56.6, 51.3, 50.8, 50.0, 39.2, 30.0 ppm; HRMS (ESI+) calcd for $C_{12}H_{15}ClO_4Na$ $[M + Na]^+$ and $[M + 2 + Na]^+$: 281.0556 and 283.0526. Found: 281.0570 and 283.0522.

(1*S,4*R**,7*S**)-5-Chloro-3,3-dimethoxy-7-ethoxybicyclo[2.2.2]oct-5-en-2-one (13c).** Yield 0.098 g (75%) as a yellowish viscous liquid; IR (KBr) ν_{max} 1742, 1619, 1449, 1361, 1105, 1029 cm^{-1}; ^{1}H NMR (500 MHz, $CDCl_3$) δ 5.99 (dd, J = 1.5, 6.5 Hz, 1H), 3.97–3.94 (m, 1H), 3.57 (dd, J = 2.5, 6.5 Hz, 1H), 3.52–3.39 (m, 2H), 3.37 (s, 3H), 3.31 (s, 3H), 3.16 (q, J = 3.0 Hz, 1H), 2.46 (ddd, J = 2.5, 8.0, 13.5 Hz, 1H), 1.56 (td, J = 3.5, 13.5 Hz, 1H), 1.17 (t, J = 7.0 Hz, 3H) ppm; ^{13}C NMR (125 MHz, $CDCl_3$) δ 199.8, 136.0, 119.4, 93.4, 74.1, 64.4, 54.6, 50.8, 49.9, 46.9, 30.6, 15.3 ppm; HRMS (ESI+) calcd for $C_{12}H_{17}ClO_4Na$ $[M + Na]^+$: 283.0713. Found: 283.0713.

(1*S,4*R**,7*S**)-7-Butyloxy-5-chloro-3,3-dimethoxybicyclo[2.2.2]oct-5-en-2-one (13d).** Yield 0.118 g (82%) as a white liquid; IR (KBr) ν_{max} 1743, 1621, 1464, 1357, 1276, 1107, 1057 cm^{-1}; ^{1}H NMR (500 MHz, $CDCl_3$) δ 5.97 (dd, J = 2.0, 6.5 Hz, 1H), 3.95–3.92 (m, 1H), 3.56 (dd, J = 2.5, 6.5 Hz, 1H), 3.44–3.40 (m, 1H), 3.36 (s, 3H), 3.35–3.33 (m, 1H), 3.32 (s, 3H), 3.15 (q, J = 3.0 Hz, 1H), 2.45 (ddd, J = 2.5, 8.0, 13.5 Hz, 1H), 1.55 (ddd, J = 3.5, 6.5, 13.5 Hz, 1H), 1.52–1.48 (m, 2H), 1.37–1.29 (m, 2H), 0.95 (t, J = 3.0 Hz, 3H) ppm; ^{13}C NMR (125 MHz, $CDCl_3$) δ 200.0, 136.0, 119.4, 93.5, 74.3, 68.9, 54.6, 50.8, 49.9, 46.9, 31.7, 30.6, 19.3, 13.8 ppm; HRMS (ESI+) calcd for $C_{14}H_{21}ClO_4Na$ $[M + Na]^+$ and $[M + 2 + Na]^+$: 311.1026 and 313.0997. Found: 311.1029 and 313.1001.

(1*R,4*R**,7*S**)-5-Chloro-3,3-dimethoxy-7-phenylthiobicyclo-[2.2.2]oct-5-en-2-one (13e).** Yield 0.134 g (83%) as a yellow semi-solid; IR (KBr) ν_{max} 1736, 1606, 1442, 1314, 1250, 1207, 1134, 1089, 1055 cm^{-1}; ^{1}H NMR (500 MHz, $CDCl_3$) δ 7.51–7.41 (m, 2H), 7.36–7.28 (m, 3H), 6.10 (apparent dd, J = 3.0, 7.0 Hz, 1H), 3.68–3.62 (m, 1H), 3.38 (s, 3H), 3.36 (s, 3H), 3.28 (apparent dd, J = 2.5, 6.5 Hz, 1H), 3.21 (d, J = 2.5 Hz, 1H), 2.60 (ddd, J = 2.5, 9.0, 13.0 Hz, 1H), 1.49 (ddd, J = 2.5, 5.0, 13.5 Hz, 1H) ppm; ^{13}C NMR (125 MHz, $CDCl_3$) δ 199.4, 136.5, 133.9, 132.1, 129.3, 127.8, 121.0, 93.6, 53.6, 50.8, 50.2, 47.6, 42.2, 28.8 ppm; HRMS (ESI+) calcd for $C_{16}H_{17}ClO_3SNa$ $[M + Na]^+$: 347.0479. Found: 347.0429.

(1*R,4*S**,8*RS*)-2-Chloro-6,6-dimethoxy-5-oxobicyclo[2.2.2]oct-2-en-8-yl acetate (13f).** Yield 0.096 g (70%) as a yellow liquid; IR (KBr) ν_{max} 2946, 1744, 1448, 1367, 1099 cm^{-1}; ^{1}H NMR (500 MHz, $CDCl_3$) δ 6.16 (dd, J = 2.5, 7.0 Hz, 1H), 6.02 (dd, J = 2.0, 6.5 Hz, 1H), 5.23–5.20 (m, 1H), 3.90 (s, 3H), 3.83 (d, J = 6.5 Hz, 1H), 3.51 (dd, J = 2.5, 6.5 Hz, 1H), 3.42–3.39 (m, 1H), 3.39 (s, 3H), 3.32 (s, 3H), 3.30 (d, J = 5.0 Hz, 1H), 3.20 (q, J = 3.0 Hz, 1H), 2.66 (ddd, J = 3.0, 8.5, 14.5 Hz, 1H), 2.04 (s, 3H), 1.57 (ddd, J = 3.5, 7.0, 14.0 Hz, 1H) ppm.

(1*S,4*R**,7*S**)-5-Bromo-3,3-dimethoxy-7-phenylbicyclo[2.2.2]oct-5-en-2-one (14a).** Yield 0.125 g (74%) as a white solid: mp 87–88 °C; IR (KBr) ν_{max} 1737, 1605, 1485, 1453, 1323, 1198, 1134, 1094, 1064 cm^{-1}; ^{1}H NMR (500 MHz, $CDCl_3$) δ 7.31–7.28 (m, 2H), 7.25–7.22 (m, 1H), 7.16–7.14 (m, 2H), 6.27 (dd, J = 2.5, 7.0 Hz, 1H), 3.42 (s, 3H), 3.40 (s, 3H), 3.35–3.30 (m, 2H), 3.25 (dd, J = 1.5, 6.5 Hz, 1H), 2.56 (ddd, J = 3.0, 9.5, 13.0 Hz, 1H), 1.84 (ddd, J = 2.5, 6.5, 13.5 Hz, 1H) ppm; ^{13}C NMR (125 MHz, $CDCl_3$) δ 199.8, 143.2, 128.7, 127.5, 127.1, 125.2, 124.9, 93.8, 57.3, 50.8, 50.2, 50.1, 40.0, 30.3 ppm; HRMS (ESI+) calcd for $C_{16}H_{17}BrO_3Na$ $[M + Na]^+$ and $[M + 2 + Na]^+$: 359.0258 and 361.0237. Found: 359.0255 and 361.0233.

(1*R,2*R**,6*R**,7*R**)-11-Bromo-8,8-dimethoxy-3-oxatricyclo-[5.2.2.0^{2,6}]undec-10-en-9-one (14b).** Yield 0.144 g (95%) as a liquid; IR (KBr) ν_{max} 1737, 1612, 1449, 1219, 1143, 1094, 1050 cm^{-1}; ^{1}H NMR (500 MHz, $CDCl_3$) δ 6.26 (ddd, J = 0.5, 2.0, 6.5, 1H), 4.33 (dd, J = 3.0, 8.0 Hz, 1H), 3.95 (dt, J = 3.5, 8.0 Hz, 1H), 3.60 (ddd, J = 2.5, 8.5, 11.5 Hz, 1H), 3.56 (dd, J = 3.5, 6.5 Hz, 1H), 3.38 (s, 3H), 3.37–3.36 (m, 1H), 3.34 (s, 3H), 3.04 (ddd, J = 2.5, 8.0, 17.0 Hz, 1H), 2.14 (dddd, J = 3.0, 6.5, 9.5, 12.5 Hz, 1H), 1.81 (dddd, J = 2.5, 9.0, 12.0, 15.5 Hz, 1H) ppm; ^{13}C NMR (125 MHz, $CDCl_3$) δ 199.2, 125.6, 122.5, 93.3, 78.0, 69.2, 56.9, 52.6, 50.9, 50.1, 39.6, 29.8 ppm; HRMS (ESI+) calcd for $C_{12}H_{15}BrO_4Na$ $[M + Na]^+$ and $[M + 2 + Na]^+$: 325.0051 and 327.0031. Found: 325.0050 and 327.0033.

(1*S,4*R**,7*S**)-5-Bromo-3,3-dimethoxy-7-ethoxybicyclo[2.2.2]oct-5-en-2-one (14c).** Yield 0.114 g (75%) as a white liquid; IR (KBr) ν_{max} 1742, 1613, 1448, 1273, 1369, 1104 cm^{-1}; ^{1}H NMR (500 MHz, $CDCl_3$) δ 6.21 (d, J = 6.5 Hz, 1H), 3.96–3.94 (m, 1H), 3.55–3.53 (m, 1H), 3.51–3.47 (m, 1H), 3.44–3.39 (m, 1H), 3.37 (s, 3H), 3.31 (s, 3H), 3.25–3.23 (m, 1H), 2.45 (ddd, J = 2.5, 8.5, 13.5 Hz, 1H), 1.55 (td, J = 3.0, 13.5 Hz, 1H), 1.17 (t, J = 7.0 Hz, 3H) ppm; ^{13}C NMR (125 MHz, $CDCl_3$); δ 199.5, 124.0, 123.9, 93.7, 74.0, 64.4, 55.8, 50.9, 50.0, 48.6, 30.7, 15.3 ppm; HRMS (ESI+) calcd for $C_{12}H_{17}BrO_4Na$ $[M + Na]^+$ and $[M + 2 + Na]^+$: 327.0207 and 329.0187. Found: 327.0212 and 329.0204.

(1*S,4*R**,7*S**)-5-Bromo-7-butyloxy-3,3-dimethoxybicyclo[2.2.2]oct-5-en-2-one (14d).** Yield 0.142 g (85%) as a white liquid; IR (KBr) ν_{max} 1743, 1614, 1460, 1360, 1105 cm^{-1}; ^{1}H NMR (500 MHz, $CDCl_3$) δ 6.20 (dd, J = 2.0, 6.5 Hz, 1H), 3.94–3.91 (m, 1H), 3.54 (dd, J = 2.5, 7.0 Hz, 1H), 3.43–3.40 (m, 1H), 3.37 (s, 3H), 3.36–3.33 (m, 1H), 3.31 (s, 3H), 3.24 (q, J = 3.0 Hz, 1H), 2.44 (ddd, J = 3.0, 8.0, 13.5 Hz, 1H), 1.54 (ddd, J = 3.0, 6.5, 13.5 Hz, 1H), 1.52–1.48 (m, 2H), 1.35–1.30 (m, 2H), 0.90 (t, J = 7.5 Hz, 3H) ppm; ^{13}C NMR (125 MHz, $CDCl_3$) δ 199.6, 124.1, 123.9, 93.7, 74.1, 68.9, 55.8, 50.9, 49.9, 48.6, 31.8, 30.7, 19.3, 13.8 ppm; HRMS (ESI+) calcd for $C_{14}H_{21}BrO_4Na$ $[M + Na]^+$ and $[M + 2 + Na]^+$: 355.0520 and 357.0499. Found: 355.0509 and 357.0490.

(1*R,4*R**,7*S**)-5-Bromo-3,3-dimethoxy-7-phenylthiobicyclo-[2.2.2]oct-5-en-2-one (14e).** Yield 0.142 g (77%) as a yellow crystalline solid: mp 110–112 °C; IR (KBr) ν_{max} 1736, 1593, 1439, 1126, 1087, 1055, 1015 cm^{-1}; ^{1}H NMR (500 MHz, $CDCl_3$) δ 7.42–7.28 (m, 5H), 6.33 (dd, J = 2.0, 7.0 Hz, 1H), 3.66–3.60 (m, 1H), 3.38 (s, 3H), 3.33 (s, 3H), 3.30 (q, J = 2.5 Hz, 1H), 3.26 (dd, J = 2.0, 6.5 Hz, 1H), 2.60 (ddd, J = 3.0, 9.5, 14.0 Hz, 1H), 1.49 (ddd, J = 3.0, 6.0, 14.0 Hz, 1H) ppm; ^{13}C NMR (125 MHz, $CDCl_3$) δ 199.2, 133.9, 132.1, 129.1, 127.9, 125.6, 124.4, 93.8, 54.7, 50.8, 50.2, 49.3, 41.9, 28.9 ppm; HRMS (ESI+) calcd for $C_{16}H_{17}SBrO_3Na$ $[M + Na]^+$ and $[M + 2 + Na]^+$: 390.9979 and 392.9958. Found: 390.9961 and 392.9931.

(1*R,4*S**,8*RS*)-2-Bromo-6,6-dimethoxy-5-oxobicyclo[2.2.2]oct-2-en-8-yl acetate (14f).** Yield 0.144 g (90%) as a viscous liquid; IR (KBr) ν_{max} 2947, 1740, 1441, 1321, 1024 cm^{-1}; ^{1}H NMR

(500 MHz, $CDCl_3$) δ 6.26 (dd, *J* = 1.5, 7.0 Hz, 1H), 6.22 (dd, *J* = 2.5, 7.5 Hz, 1H), 5.20 (m, 1H), 5.06 (m, 1H), 3.48 (dd, *J* = 2.5, 6.5 Hz, 1H), 3.40 (s, 3H), 3.39 (s, 3H), 3.37 (s, 3H), 3.31 (s, 3H), 3.30 (m, 1H), 3.28 (m, 1H), 2.65 (ddd, *J* = 3.0, 8.5, 14.0 Hz, 1H), 2.25 (ddd, *J* = 3.5, 10.0, 14.5 Hz, 1H), 2.04 (s, 3H), 2.03 (s, 3H), 1.94 (ddd, *J* = 2.0, 6.5, 14.0 Hz, 1H), 1.57 (ddd, *J* = 3.5, 6.5, 14.0 Hz, 1H) ppm.

(1*S,4*R**,7*S**)-3,3-Dimethoxy-5-iodo-7-phenylbicyclo[2.2.2]-oct-5-en-2-one (15a).** Yield 0.144 g (75%) as a white solid: mp 68–69 °C; IR (KBr) ν_{max} 1736, 1593, 1452, 1260, 1197, 1133, 1091 cm^{-1}; ^1H NMR (500 MHz, $CDCl_3$) δ 7.31–7.22 (m, 3H), 7.15–7.13 (m, 2H), 6.59 (dd, *J* = 2.0, 7.0 Hz, 1H), 3.45 (q, *J* = 2.5 Hz, 1H), 3.42 (s, 3H), 3.40 (s, 3H), 3.39–3.35 (m, 1H), 3.15 (dd, *J* = 1.5, 6.5 Hz, 1H), 2.48 (ddd, *J* = 3.0, 9.5, 13.0 Hz, 1H), 1.81 (ddd, *J* = 2.5, 6.5, 13.5 Hz, 1H) ppm; ^{13}C NMR (125 MHz, $CDCl_3$) δ 199.6, 143.3, 134.2, 128.7, 127.5, 127.0, 95.9, 94.0, 58.8, 53.1, 51.0, 50.2, 39.8, 30.1 ppm; HRMS (ESI+) calcd for $C_{16}H_{17}IO_3Na$ $[M + Na]^+$: 407.0120. Found: 407.0119.

(1*R,2*R**,6*R**,7*R**)-8,8-Dimethoxy-11-iodo-3-oxatricyclo-[5.2.2.0^{2,6}]undec-10-en-9-one (15b).** Yield 0.149 g (85%) as a white solid: mp 72–73 °C; IR (KBr) ν_{max} 1735, 1590, 1451, 1349, 1275, 1139 cm^{-1}; ^1H NMR (500 MHz, $CDCl_3$) δ 6.61 (dd, *J* = 1.0, 6.5 Hz, 1H), 4.35 (dd, *J* = 3.0, 8.0 Hz, 1H), 3.95 (dt, *J* = 3.5, 8.5 Hz, 1H), 3.63–3.59 (m, 1H), 3.51 (dd, *J* = 3.0, 6.5 Hz, 1H), 3.48–3.47 (m, 1H), 3.38 (s, 3H), 3.33 (s, 3H), 3.12–3.06 (m, 1H), 2.13 (dddd, *J* = 3.5, 6.5, 10.0, 13.0 Hz, 1H), 1.96–1.87 (m, 1H) ppm; ^{13}C NMR (125 MHz, $CDCl_3$) δ 199.0, 134.5, 93.6, 93.1, 77.9, 69.3, 58.5, 54.7, 51.2, 50.0, 39.9, 29.4 ppm; HRMS (ESI+) calcd for $C_{12}H_{15}IO_4Na$ $[M + Na]^+$: 372.9912. Found: 372.9908.

(1*S,4*R**,7*S**)-3,3-Dimethoxy-7-ethoxy-5-iodobicyclo[2.2.2]oct-5-en-2-one (15c).** Yield 0.153 g (87%) as a white viscous liquid; IR (KBr) ν_{max} 1741, 1594, 1447, 1358, 1272, 1103, 1047 cm^{-1}; ^1H NMR (500 MHz, $CDCl_3$) δ 6.53 (dd, *J* = 1.5, 7.0 Hz, 1H), 3.96–3.93 (m, 1H), 3.52–3.39 (m, 3H), 3.37 (s, 3H), 3.30 (s, 3H), 3.28–3.27 (m, 1H), 2.38 (ddd, *J* = 3.0, 8.5, 14.0 Hz, 1H), 1.52 (td, *J* = 3.0, 13.5 Hz, 1H), 1.17 (t, *J* = 7.0 Hz, 3H) ppm; ^{13}C NMR (125 MHz, $CDCl_3$) δ 199.2, 132.8, 94.7, 93.8, 73.8, 64.3, 57.2, 51.3, 51.0, 49.9, 30.4, 15.2 ppm; HRMS (ESI+) calcd for $C_{12}H_{17}IO_4Na$ $[M + Na]^+$: 375.0069. Found: 375.0060.

(1*S,4*R**,7*S**)-7-Butyloxy-3,3-dimethoxy-5-iodobicyclo[2.2.2]-oct-5-en-2-one (15d).** Yield 0.167 g (88%) as a viscous liquid; IR (KBr) ν_{max} 1742, 1596, 1459, 1360, 1268, 1103, 1056 cm^{-1}; ^1H NMR (500 MHz, $CDCl_3$) δ 6.52 (dd, *J* = 1.5, 6.5 Hz, 1H), 3.95–3.90 (m, 1H), 3.45 (dd, *J* = 2.5, 7.0 Hz, 1H), 3.42–3.39 (m, 1H), 3.37 (s, 3H), 3.36–3.30 (m, 1H), 3.30 (s, 3H), 3.27 (q, *J* = 3.0 Hz, 1H), 2.36 (ddd, *J* = 3.0, 8.0, 14.0 Hz, 1H), 1.53–1.48 (m, 3H), 1.37–1.30 (m, 2H), 0.90 (t, *J* = 7.5 Hz, 3H) ppm; ^{13}C NMR (125 MHz, $CDCl_3$) δ 199.4, 132.9, 94.7, 93.9, 74.0, 68.9, 57.2, 51.4, 51.1, 49.9, 31.7, 30.5, 19.3, 13.8 ppm; HRMS (ESI+) calcd for $C_{14}H_{21}IO_4Na$ $[M + Na]^+$: 403.0382. Found: 403.0377.

(1*R,4*R**,7*S**)-3,3-Dimethoxy-5-iodo-7-phenylthiobicyclo[2.2.2]-oct-5-en-2-one (15e).** Yield 0.189 g (91%) as a yellow solid: mp 101–103 °C; IR (KBr) ν_{max} 1726, 1583, 1441, 1310, 1252, 1205, 1131, 1078, 1051 cm^{-1}; ^1H NMR (500 MHz, $CDCl_3$) δ 7.43–7.40 (m, 2H), 7.37–7.30 (m, 3H), 6.66 (dd, *J* = 1.5, 6.5 Hz, 1H), 3.66–3.24 (m, 1H), 3.41 (s, 3H), 3.37–3.35 (m, 1H), 3.35 (s, 3H), 3.20 (dd, *J* = 2.0, 6.5 Hz, 1H), 2.54 (ddd, *J* = 3.0, 9.5, 17.0 Hz, 1H), 1.48 (ddd, *J* = 3.0, 5.5, 17.0 Hz, 1H) ppm; ^{13}C NMR (125 MHz, $CDCl_3$) δ 199.0, 134.5, 133.9, 132.1, 129.3, 127.8, 95.3, 94.0, 56.2, 52.3, 51.1, 50.2, 41.8, 28.7 ppm; HRMS (ESI+) calcd for $C_{16}H_{17}IO_3SNa$ $[M + Na]^+$: 438.9835. Found: 438.9812.

(1*R,4*S**,8*RS*)-2-Iodo-6,6-dimethoxy-5-oxobicyclo[2.2.2]oct-2-en-8-yl acetate (15f).** Yield 0.165 g (90%) as a viscous liquid; IR (KBr) ν_{max} 2946, 1742, 1436, 1370, 1097 cm^{-1}; ^1H NMR (500 MHz, $CDCl_3$) δ 6.58 (dd, *J* = 1.5, 6.5 Hz, 1H), 6.02 (dd, *J* = 2.0, 6.5 Hz, 1H), 5.20 (m, 1H), 5.04 (m, 1H), 3.40–3.39 (m, 1H), 3.39 (s, 3H), 3.38 (s, 3H), 3.38–3.37 (m, 1H), 3.36 (s, 3H), 3.35–3.31 (m, 3H), 3.30 (s, 3H), 2.57 (ddd, *J* = 2.5, 8.0, 14.0 Hz, 1H), 2.22 (ddd, *J* = 3.0, 10.0, 14.0 Hz, 1H), 2.04 (s, 3H), 2.03 (s, 3H), 1.87 (ddd, *J* = 2.5, 5.0, 14.5 Hz, 1H), 1.53 (ddd, *J* = 3.5, 7.0, 14.5 Hz, 1H) ppm.

Acknowledgements

Thanks are due to Mr Virendra Singh Rajora for carrying out a couple of reactions presented herein. We are grateful to DST, New Delhi for financial support (research grant no. SR/S1/OC-38/2011) and HRMS facility (DST-FIST program). SRS and SKRP thank CSIR, New Delhi for the award of research fellowships.

Notes and references

1 (*a*) S. P. Roche and J. A. Porco Jr., *Angew. Chem., Int. Ed.*, 2011, **50**, 4068–4093; (*b*) L. Pouységu, D. Deffieux and S. Quideau, *Tetrahedron*, 2010, **66**, 2235–2261; (*c*) S. Quideau, L. Pouységu and D. Deffieux, *Synlett*, 2008, 467–495.

2 (*a*) D. Magdziak, S. J. Meek and T. R. R. Pettus, *Chem. Rev.*, 2004, **104**, 1383–1429; (*b*) S. Quideau and L. Pouysegu, *Org. Prep. Proced. Int.*, 1999, **31**, 617–680; (*c*) V. Singh, *Acc. Chem. Res.*, 1999, **32**, 324–333.

3 (*a*) C.-C. Liao, *Pure Appl. Chem.*, 2005, **77**, 1221–1234; (*b*) C.-C. Liao and R. K. Peddinti, *Acc. Chem. Res.*, 2002, **35**, 856–866.

4 D.-S. Hsu, P.-Y. Hsu and C.-C. Liao, *Org. Lett.*, 2001, **3**, 263–265.

5 C.-F. Yen and C.-C. Liao, *Angew. Chem., Int. Ed.*, 2002, **41**, 4090–4093.

6 D.-S. Hsu, P.-Y. Hsu and C.-C. Liao, *Org. Lett.*, 2003, **5**, 4741–4743.

7 (*a*) P.-Y. Hsu, R. K. Peddinti, S. K. Chittimalla and C.-C. Liao, *J. Org. Chem.*, 2005, **70**, 9156–9167; (*b*) C.-H. Chen, R. K. Peddinti, N. S. K. Rao and C.-C. Liao, *J. Org. Chem.*, 2004, **69**, 5365–5375.

8 D.-S. Hsu and C.-C. Liao, *Org. Lett.*, 2007, **9**, 4563–4565.

9 D.-S. Hsu, P.-Y. Hsu, Y.-C. Lee and C.-C. Liao, *J. Org. Chem.*, 2008, **73**, 2554–2563.

10 H.-Y. Shiao, H.-P. Hsieh and C.-C. Liao, *Org. Lett.*, 2008, **10**, 449–452.

11 P.-H. Lu, C.-S. Yang, B. Devendar and C.-C. Liao, *Org. Lett.*, 2010, **12**, 2642–2645.

12 S. A. Snyder and F. Kotes, *J. Am. Chem. Soc.*, 2009, **131**, 1745–1752.

13 H. E. Zimmerman and D. Armesto, *Chem. Rev.*, 1996, **96**, 3065–3112.

14 C.-C. Liao, C.-S. Chu, T.-H. Lee, P. D. Rao, S. Ko, L.-D. Song and H.-C. Shiao, *J. Org. Chem.*, 1999, **64**, 4102–4110.

15 (*a*) H.-F. Hou, R. K. Peddinti and C.-C. Liao, *Org. Lett.*, 2002, **4**, 2477–2480; (*b*) C.-F. Yen, R. K. Peddinti and C.-C. Liao, *Org. Lett.*, 2000, **2**, 2909–2912; (*c*) G. Anderson, *Acta Chem.*, 1976, **30**, 403–406.

16 (*a*) L. Pouységu, S. Chassaing, D. Deffieux, A.-M. Lamidey, K. Miqueu, J.-M. Sotiropoulos and S. Quideau, *Angew. Chem., Int. Ed.*, 2008, **47**, 3552–3555; (*b*) C.-H. Lai, P.-Y. Lin, R. K. Peddinti and C.-C. Liao, *Synlett*, 2002, 1520–1522; (*c*) A. S. Mitchell and R. A. Russell, *Tetrahedron*, 1997, **53**, 4387–4410.

17 (*a*) G. Andersson and P. Berntsson, *Acta Chem. Scand. Ser. B*, 1975, **29**, 948–952; (*b*) H. D. Becker, T. Bremholt and E. Adler, *Tetrahedron Lett.*, 1972, 4205–4208.

18 T. B. Patrick, H. Yu, D. Taylor and K. Gorrell, *J. Fluorine Chem.*, 2004, **125**, 1965–1966.

19 (*a*) J. Gagnepain, R. Mereau, D. Dejugnac, J.-M. Leger, F. Castet, D. Deffieux, L. Pouysegu and S. Quideau, *Tetrahedron*, 2007, **63**, 6493–6505; (*b*) S. Quideau, I. Fabre and D. Deffieux, *Org. Lett.*, 2004, **6**, 4571–4573; (*c*) S. Quideau, L. Pouységu, D. Deffieux, A. Ozanne, J. Gagnepain, I. Fabre and M. Oxoby, *ARKIVOC*, 2003, **6**, 106–119.

20 (*a*) S. K. R. Parumala and R. K. Peddinti, *Org. Lett.*, 2013, **15**, 3546–3549; (*b*) S. R. Surasani and R. K. Peddinti, *Tetrahedron Lett.*, 2011, **52**, 4615–4618; (*c*) S. R. Surasani, V. S. Rajora, N. Bodipati and R. K. Peddinti, *Tetrahedron Lett.*, 2009, **50**, 773–775.

21 S. K. Chittimalla and C.-C. Liao, *Tetrahedron*, 2003, **59**, 4039–4046.

22 (*a*) S.-Y. Gao, S. K. Chittimalla, G. J. Chuang and C.-C. Liao, *J. Org. Chem.*, 2009, **74**, 1632–1639; (*b*) S.-Y. Gao, S. Ko, Y.-L. Lin, R. K. Peddinti and C.-C. Liao, *Tetrahedron*, 2001, **57**, 297–308; (*c*) S.-Y. Gao, Y.-L. Lin, P. D. Rao and C.-C. Liao, *Synlett*, 2000, 421–423; (*d*) O. Arjona, R. Medel and J. Plumet, *Tetrahedron Lett.*, 1999, **40**, 8431–8433.

23 (*a*) M. Avalos, R. Babiano, N. Cabello, P. Cintas, M. B. Hursthouse, J. L. Jiménez, M. E. Light and J. C. Palacios, *J. Org. Chem.*, 2003, **68**, 7193–7203; (*b*) C.-S. Chu, T.-H. Lee and C.-C. Liao, *Synlett*, 1994, 635–636.

24 M. J. Frisch, G. W. Trucks, H. B. Schlegel, G. E. Scuseria, M. A. Robb, J. R. Cheeseman, G. Scalmani, V. Barone, B. Mennucci, G. A. Petersson, H. Nakatsuji, M. Caricato, X. Li, H. P. Hratchian, A. F. Izmaylov, J. Bloino, G. Zheng, J. L. Sonnenberg, M. Hada, M. Ehara, K. Toyota, R. Fukuda, J. Hasegawa, M. Ishida, T. Nakajima, Y. Honda, O. Kitao, H. Nakai, T. Vreven, J. A. Montgomery Jr., J. E. Peralta, F. Ogliaro, M. Bearpark, J. J. Heyd, E. Brothers, K. N. Kudin, V. N. Staroverov, R. Kobayashi, J. Normand, K. Raghavachari, A. Rendell, J. C. Burant, S. S. Iyengar, J. Tomasi, M. Cossi, N. Rega, N. J. Millam, M. Klene, J. E. Knox, J. B. Cross, V. Bakken, C. Adamo, J. Jaramillo, R. Gomperts, R. E. Stratmann, O. Yazyev, A. J. Austin, R. Cammi, C. Pomelli, J. W. Ochterski, R. L. Martin, K. Morokuma, V. G. Zakrzewski, G. A. Voth, P. Salvador, J. J. Dannenberg, S. Dapprich, A. D. Daniels, O. Farkas, J. B. Foresman, J. V. Ortiz, J. Cioslowski and D. J. Fox, *Gaussian 09, Revision A.02*, Gaussian, Inc., Wallingford, CT, 2009.

25 (*a*) C. Lee, W. Yang and R. G. Parr, *Phys. Rev. B: Condens. Matter*, 1988, **37**, 785–789; (*b*) A. D. Becke, *J. Chem. Phys.*, 1993, **98**, 5648–5652; (*c*) W. Kohn, A. D. Becke and R. G. Parr, *J. Phys. Chem.*, 1996, **100**, 12974–12980.

26 W. J. Hehre, L. Radom, P. V. R. Schleyer and J. A. Pople, *Ab initio Molecular Orbital Theory*, Wiley, New York, 1986.

27 (*a*) E. Goldstein, B. Beno and K. N. Houk, *J. Am. Chem. Soc.*, 1996, **118**, 6036–6043; (*b*) O. Wiest, D. C. Montiel and K. N. Houk, *J. Phys. Chem. A*, 1997, **101**, 8378–8388; (*c*) J. I. García, V. Martínez-Merino, J. A. Mayoral and L. Salvatella, *J. Am. Chem. Soc.*, 1998, **120**, 2415–2420; (*d*) D. M. Birney, *J. Am. Chem. Soc.*, 2000, **122**, 10917–10925.

28 O. Arjona, R. Medel, J. Plumet, R. Herrera, H. A. Jiménez-Vázquez and J. Tamariz, *J. Org. Chem.*, 2004, **69**, 2348–2354.

29 (*a*) Y. L. Dory, A.-L. Roy, P. Soucy and P. Deslongchamps, *Org. Lett.*, 2009, **11**, 1197–1200; (*b*) L. R. Domingo and M. J. Aurell, *J. Org. Chem.*, 2002, **67**, 959–965.

30 (*a*) T. C. Dinadayalane, R. Vijaya, A. Smitha and G. N. Sastry, *J. Phys. Chem. A*, 2002, **106**, 1627–1633; (*b*) E. G. Bengoa, M. D. Helm, A. Plant and J. P. A. Harrity, *J. Am. Chem. Soc.*, 2007, **129**, 2691–2699.

31 J. I. García, J. A. Mayoral and L. Salvatella, *Acc. Chem. Res.*, 2000, **33**, 658–664.

32 (*a*) R. G. Parr and R. G. Pearson, *J. Am. Chem. Soc.*, 1983, **105**, 7512–7516; (*b*) R. G. Parr and W. Yang, *Density Functional Theory of Atoms and Molecules*, Oxford University Press, New York, 1989.